Boise Climate Adaptation Assessment (BCAA): Building Climate Readiness in Boise

Metric I: Heat stress days

Metric II: Heavy precipitation days

Metric III: Irrigation demand

Metric IV: Summer drought

Metric V: Wildfire and smoke potential

Metric VI: Seasonal Streamflow

Metric VII: High streamflow and river flooding potential

Metric VIII: Low streamflow and water quality

General overview of projected changes in climate for Boise

Projected changes in climate for the Boise metropolitan area resemble those across much of the broader interior northwestern United States including notable warming across all seasons and a slight increase in annual precipitation (e.g., Rupp et al., 2016; Mote et al., 2014). There is some uncertainty across models regarding future changes in precipitation. However, a vast majority of models suggest that precipitation will remain unchanged or increase slightly. A couple of the 20 models that were examined showed minor decreases in annual precipitation. Average model increases in precipitation are rather small and range between 5-10% for the early and mid-21st century. Notably, these changes are small in comparison to the observed annual and decadal variability observed in the region for the past century. By contrast, projected increases in temperature are large relative to the historical annual and decadal variability and will likely result in average years by the mid-21st century being warmer than any year observed in Boise over the past century.

Seasonal variations in projected changes in climate are anticipated as shown in Figure A. The largest rates of warming of 8-9°F are anticipated during the summer months (Jul-Sep) by the mid-to-late 21st century. Likewise, the increase in precipitation is projected to predominantly be during the cool season from November-April, with nominal changes during the warm months of the year. However, we note that there is some level of uncertainty regarding projected changes in precipitation due to inadequacies in global climate models resolving orographic precipitation germane to much of the region (e.g. Luce et al., 2013).

Relatively minor changes in annual precipitation contrasted with robust increases in temperature will bring about substantial changes in seasonal water availability (Mote et al., 2014). Notably, with more precipitation falling as rain rather than snow across mountain watersheds, runoff will commence earlier in the year and leave less snow to melt and replenish streams in the summer months when precipitation in scant. Furthermore, warming will increase the water demand from vegetation resulting in more acute drought stress on ecosystems and streams during the summer months that is likely to manifest through increased fire risk and critically low summer streamflow.

This report uses the latest climate science to assess a set of eight climate related impacts identified by the City of Boise. The report draws on a set of 20 downscaled climate models from a broader set of climate models used in the Intergovernmental Panel on Climate Change's Fifth Assessment Report and the National Climate Assessment. These data were downscaled by Dr. John Abatzoglou's research group at the University of Idaho and publically available at http://maca.northwestknowledge.net.

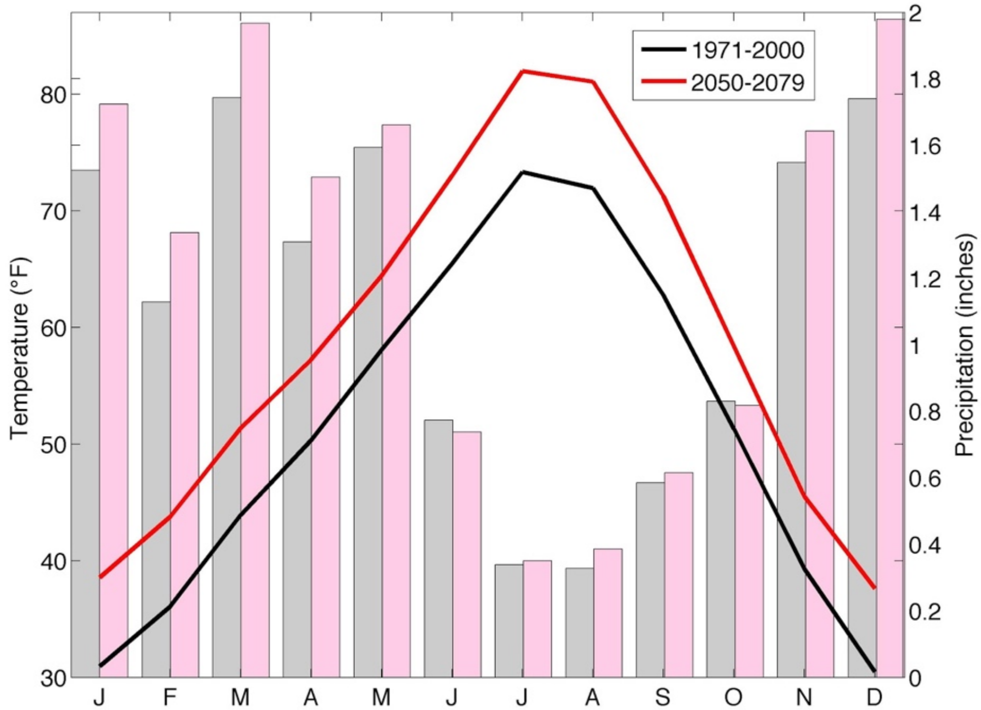

Figure A: Climograph showing monthly mean temperature (lines) and precipitation (bars) for Boise, Idaho for late-20th century averages (1971-2000, black) and mid-21st century (2050-2079, red) projections for the high emissions scenario (RCP 8.5). The average response from 20 climate projections is shown to simplify the visual.

<u>References</u>

Luce, C. H., J. T. Abatzoglou, and Z. A. Holden, 2013. The missing mountain water: Slower westerlies decrease orographic enhancement in the Pacific Northwest USA, *Science*, 342(6164), 1360–1364

Mote, P., A.K. Snover, S. Capalbo, S.D. Eigenbrode, P. Glick, J. Littell, R. Raymondi, and S. Reeder, 2014. Ch. 21: Northwest. Climate Change Impacts in the United States: The Third National Climate Assessment, J. M. Melillo, Terese (T.C.) Richmond, and G. W. Yohe, Eds., U.S. Global Change Research Program, 495-521.

Rupp, D.E., Abatzoglou, J.T. and Mote, P.W., 2016. Projections of 21st century climate of the Columbia River Basin. *Climate Dynamics*, pp.1-17.

Metric I: Heat stress days

Defined: Days when the heat index exceeds 91F, as defined by the US Department of Labor as the lower limit for Occupational Heat Exposure. Such temperatures can result in elevated risk of heat-related illnesses for outdoor workers. Similarly, days with high temperatures have increased electrical demand for air conditioning that can lead to power surges. Exceptional heat also often requires cooling centers to be opened to provide relief for homeless populations.

How it is calculated: Heat Index was calculated using the Heat Index equation currently used by the National Weather Service (NWS, 2011) that incorporates temperature and relative humidity. Daily peak heat index was calculated using daily maximum temperature and calculating relative humidity by assuming no diurnal cycle in dewpoint temperature. In a dry summer climate like Boise where relative humidity is typically low, the heat index is often less than the actual temperature. Exceptions are days with elevated dewpoint temperatures. Per OSHA, Moderate Risk occurs with Heat Index values between 91-103F, and High Risk occurs with Heat Index values between 103-115F.

Data: Both daily maximum temperature and dewpoint temperature data were obtained from 20 downscaled climate models (Table 1.1) for a ~2.5 mile by 2.5 mile grid point centered over Boise, Idaho (43.61°N, 116.2°W). These data were downscaled using the Multivariate Adaptive Constructed Analogs (MACA, Abatzoglou and Brown, 2012) statistical downscaling method that applies observational relationships between fine-scale and coarse resolution meteorology to the coarse resolution output of global climate models. The gridded observational dataset of Abatzoglou (2013) from 1979-2016 was used as the training data. These data are not intended to provide fine-scale information on climate at the scales of individual buildings, parks, or neighborhoods -- all of which have their own microclimate, but rather a broader scale representation of climate experienced throughout the Boise metropolitan area.

Analysis: The average number of days per year with Moderate and High Risk for Heat Exposure were calculated for both the historical observed record (1979-2015), historical modeled data (1950-2005) and future climate scenarios for the early (2020-2049) and mid-21st century (2050-2079). The average number of days per heat with Heat Index values exceeding the two aforementioned thresholds is summarized over a 30-year period yielding an expected value per year. However, due to climate variability, the number of Moderate and High Risk days can vary substantially under historical and future climate.

Results: The average number of Moderate Risk and High Risk days per year in Boise, ID from 1981-2010 was 16.1 and 0.07 (Table 1.1 and 1.2). Of note is the high amount of year-to-year variability in the number of Moderate Risk days, with 1993 observing a single day, whereas at least 28 days per year of Moderate Risk were seen in 1998, 2003, 2007 and 2012. A total of 4 High Risk days were seen over the past 38 years in Boise, and have hence historically been quite rare.
Climate change projections call for a substantial increase in the frequency of Moderate Risk and High Risk days by the early and mid 21st century, particularly under the high-emissions scenario for the mid-21st century. The frequency of Moderate Risk days is projected to more than double by the early 21st century (2020-2049) with the multi-model mean of 40 and 41 days per year

under the low and high emissions scenario. A continuation of this increase to 50 and 66 days per year under the low and high emission scenario, respectively, is projected by the mid-21st century (2050-2079). Notably, these projections suggest that the average year by 2020-2049 will have a greater incidence of Moderate Risk days than any year from 1979-2016. There is a substantial amount of variability across model results; however, all models suggest at least a doubling in the frequency of Moderate Risk days by the early-21st century, with a couple models projecting near 50 days per year.

The occurrence of High Risk days is relative small by the early-21st century, with a multi-model average of 1 and 1.7 days per year for the low and high emission scenario, respectively. However, by the mid-21st century, such days become increasing common with an average of 3.7 and 11.4 days per year under the low and high emissions scenario, respectively.

Summary: The frequency of Moderate Risk days for heat extremes will increase from a historical baseline of around 16 days per summer to 41 and 66 days per summer by the early and mid-21st century under high emissions scenarios, respectively. High Risk days have been exceedingly rare in Boise; however, such days will become more common during the early and mid 21st century.

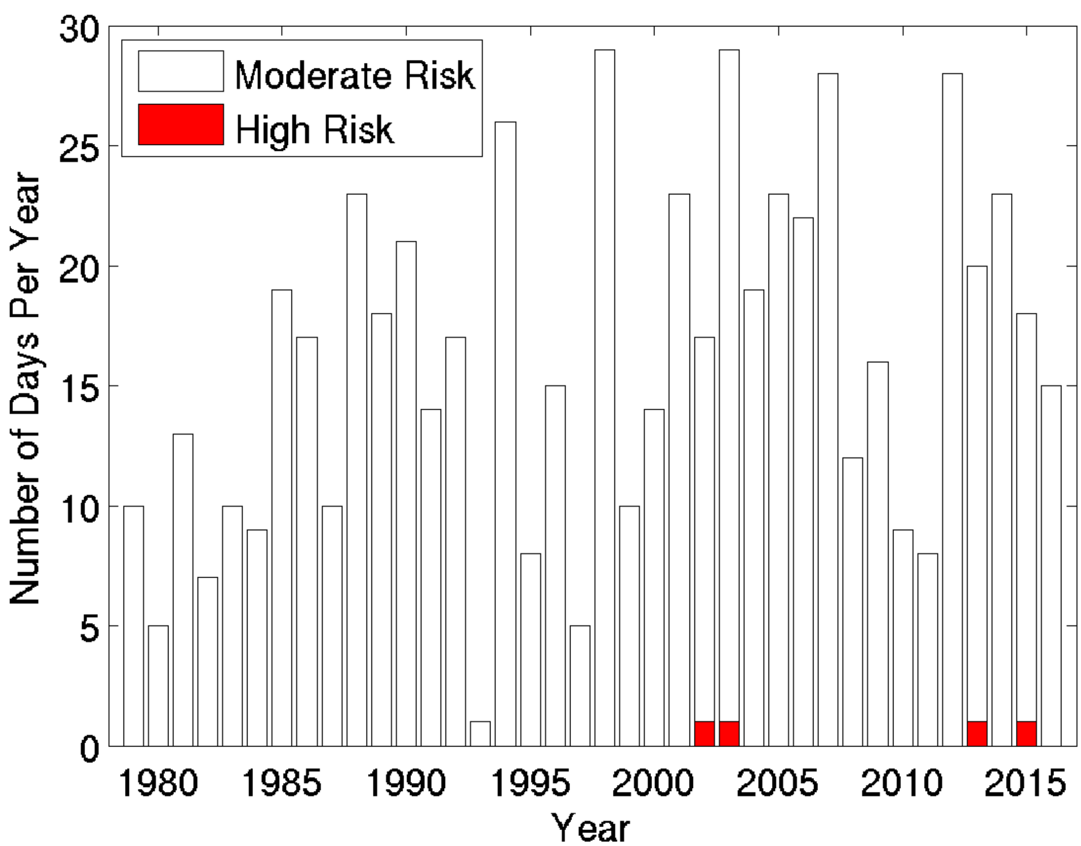

Figure 1: The number of Moderate Risk (white) and High Risk (red) days per year observed in Boise, ID from 1979-2016. Data from the gridded meteorological dataset of Abatzoglou (2013). The average number of Moderate Risk days per year from 1981-2010 was 16.1, while the number of High Risk days was 0.07.

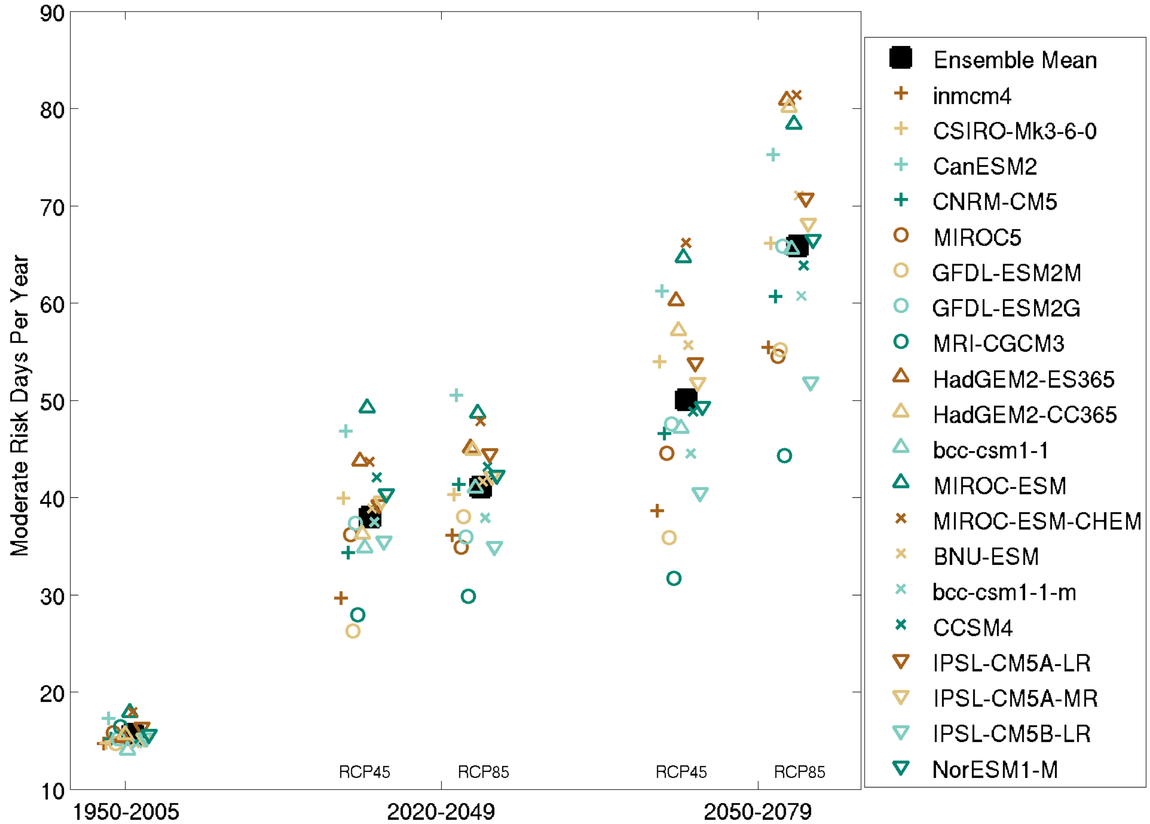

Figure 1.2: Modeled average number of Moderate Risk days per year under historical (left), early 21st century (middle) and mid-21st century (right) from 20 downscaled climate models for low emissions (RCP4.5) and high emissions (RCP8.5) scenarios. The black box shows the average of the 20 models.

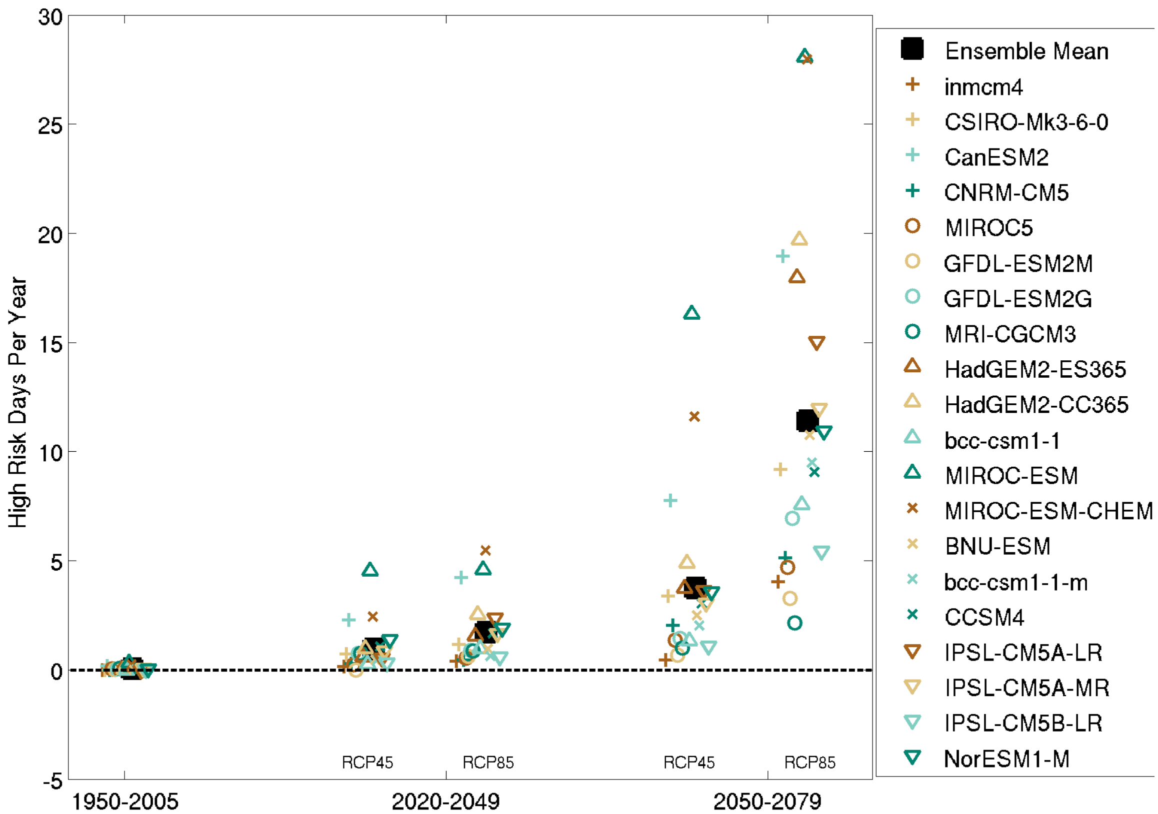

Figure 1.3: Modeled average number of High Risk days per year under historical (left), early 21st century (middle) and mid-21st century (right) from 20 downscaled climate models for low emissions (RCP4.5) and high emissions (RCP8.5) scenarios. The black box shows the average of the 20 models.

Table 1.1: Average number of Moderate Risk days (Heat Index >91F) per year for different models (rows) and time period/scenarios (columns).

	1950-2005	2020-2049 RCP45	2020-2049 RCP85	2050-2079 RCP45	2050-2079 RCP45
inmcm4	14.7	29.7	36.1	38.7	55.4
CSIRO-Mk3-6-0	14.8	40.0	40.3	54.0	66.2
CanESM2	17.3	46.8	50.5	61.2	75.3
CNRM-CM5	15.2	34.4	41.3	46.6	60.7
MIROC5	15.8	36.2	34.9	44.6	54.5
GFDL-ESM2M	14.7	26.3	38.0	35.9	55.2
GFDL-ESM2G	15.2	37.4	35.9	47.6	65.9
MRI-CGCM3	16.4	28.0	29.9	31.7	44.3
HadGEM2-ES365	15.3	43.7	45.1	60.3	80.8
HadGEM2-CC365	15.6	36.2	44.9	57.2	80.1
bcc-csm1-1	14.0	34.8	41.0	47.1	65.6
MIROC-ESM	17.9	49.2	48.7	64.7	78.4
MIROC-ESM-CHEM	17.9	43.7	47.8	66.2	81.4
BNU-ESM	14.7	38.9	41.6	55.7	71.1
bcc-csm1-1-m	14.7	37.5	37.9	44.5	60.7
CCSM4	15.2	42.1	43.1	48.8	63.9
IPSL-CM5A-LR	16.4	39.2	44.5	53.9	70.8
IPSL-CM5A-MR	15.3	39.6	42.2	51.8	68.2
IPSL-CM5B-LR	15.3	35.5	35.0	40.5	51.9
NorESM1-M	15.7	40.4	42.3	49.4	66.5
MEAN	**15.6**	**38.0**	**41.1**	**50.0**	**65.8**

Table 1.2: Average number of High Risk days (Heat Index >103F) per year for different models (rows) and time period/scenarios (columns).

	1950-2005	2020-2049 RCP45	2020-2049 RCP85	2050-2079 RCP45	2050-2079 RCP45
inmcm4	0.0	0.2	0.4	0.5	4.0
CSIRO-Mk3-6-0	0.0	0.7	1.2	3.4	9.2
CanESM2	0.2	2.3	4.2	7.8	19.0
CNRM-CM5	0.0	0.3	0.5	2.0	5.1
MIROC5	0.1	0.2	0.5	1.4	4.7
GFDL-ESM2M	0.0	0.0	0.6	0.7	3.3
GFDL-ESM2G	0.0	0.8	0.9	1.4	6.9
MRI-CGCM3	0.1	0.8	0.9	1.0	2.2
HadGEM2-ES365	0.0	0.6	1.6	3.7	18.0
HadGEM2-CC365	0.0	1.0	2.5	4.9	19.7
bcc-csm1-1	0.0	0.3	1.0	1.3	7.6
MIROC-ESM	0.3	4.5	4.6	16.3	28.1
MIROC-ESM-CHEM	0.3	2.4	5.5	11.6	28.0
BNU-ESM	0.0	0.5	1.0	2.5	10.8
bcc-csm1-1-m	0.0	0.5	0.6	2.0	9.5
CCSM4	0.0	1.1	1.7	3.0	9.1
IPSL-CM5A-LR	0.0	0.5	2.4	3.6	15.0
IPSL-CM5A-MR	0.1	0.9	1.7	3.1	12.0
IPSL-CM5B-LR	0.0	0.3	0.6	1.1	5.4
NorESM1-M	0.1	1.4	1.9	3.6	10.9
MEAN	**0.1**	**1.0**	**1.7**	**3.7**	**11.4**

<u>References</u>

Abatzoglou, J.T., and T.J. Brown. 2012, A Comparison of Statistical Downscaling Methods Suited for Wildfire Applications, International Journal of Climatology, doi:10.1002/joc.2312

Abatzoglou, J.T., 2013, Development of gridded surface meteorological data for ecological applications and modeling, International Journal of Climatology, doi: 10.1002/joc.3413

National Weather Service, 2011, Heat Index Calculation
http://www.srh.noaa.gov/images/epz/wxcalc/heatIndex.pdf

Metric II: Heavy precipitation days

Defined: Days with an excessive amount of precipitation that occur in an urban environment that exceed the capacity of stormwater and sewage systems. Excessive precipitation can lead to flood related hazards including impacts to property, roadways and water contamination. Note that flooding of this type differs from flood waters from snow-melt and/or precipitation in upstream watersheds that lead to high river flow in the Boise River.

How it is calculated: Rule curves exist for estimating flooding; however, these can vary by location and drainage and a function of duration of precipitation (e.g., 1-hour, 6-hour, 24-hour). To circumvent these challenges and make use of the daily summarized precipitation data available, a daily precipitation amount exceeding 0.7" is considered. Daily precipitation totals of this magnitude have been recorded approximately 35 times from 1979-2015 at the Boise Airport, and approximates the 1-year return period of 24-hour maximum precipitation.

Data: Daily accumulated precipitation data were obtained from 20 downscaled climate models (Table 2.1) for a ~2.5 mile by 2.5 mile grid point centered over Boise, Idaho (43.61°N, 116.2°W). These data were downscaled using the Multivariate Adaptive Constructed Analogs (MACA, Abatzoglou and Brown, 2012) statistical downscaling method that applies observational relationships between fine-scale and coarse resolution meteorology to the coarse resolution output of global climate models. The gridded observational dataset of Abatzoglou (2013) from 1979-2016 was used as the training data. These data are not intended to provide fine-scale information on climate at the scales of individual buildings, parks, or neighborhoods -- all of which have their own microclimate, but rather a broader scale representation of climate experienced throughout the Boise metropolitan area.

Analysis: The average number of days per year with heavy precipitation exceeding 0.7 inches was calculated for both the historical observed record (1979-2015), historical modeled data (1950-2005) and future climate scenarios for the early (2020-2049) and mid-21st century (2050-2079).

Results: The average number of heavy precipitation (daily accumulation >0.7 inches) in Boise, ID from 1981-2010 was 0.72. Comparable frequency was seen for the historical downscaled climate runs from 1950-2005. By the early 21st century (2020-2049) a slight increase in the frequency of such events are evident in most of the model simulations. The annual frequency of precipitation exceeding 0.7" increases to 1.04 and 1.15 times in the multi-model mean under the low and high emission scenario, respectively. The increase is more apparent by the mid-21st century, particularly under the high emissions scenario. By the mid-21st century, the annual frequency increases to 1.19 and 1.42 times in the multi-model mean under the low and high emission scenario, respectively. The latter represents an approximate doubling in the historical frequency of heavy precipitation. However, it is worthwhile to note the diversity of model results for any given time period and scenario. For example, for the mid-21st century high-emissions runs, four models show negligible change from the historical period (0.7 to 0.83 times per year), whereas three models show a tripling in the frequency of such events.

Summary: The occurrence of heavy precipitation events is projected to increase in Boise with human-caused climate change. Daily accumulated precipitation exceeding 0.7" is projected to increase by approximately 50% by the early 21st century and up to double historical frequency by the mid-21st century under high emissions scenario. There is a larger amount of uncertainty with this projection than for projections based on temperature, as not all models show a significant increase.

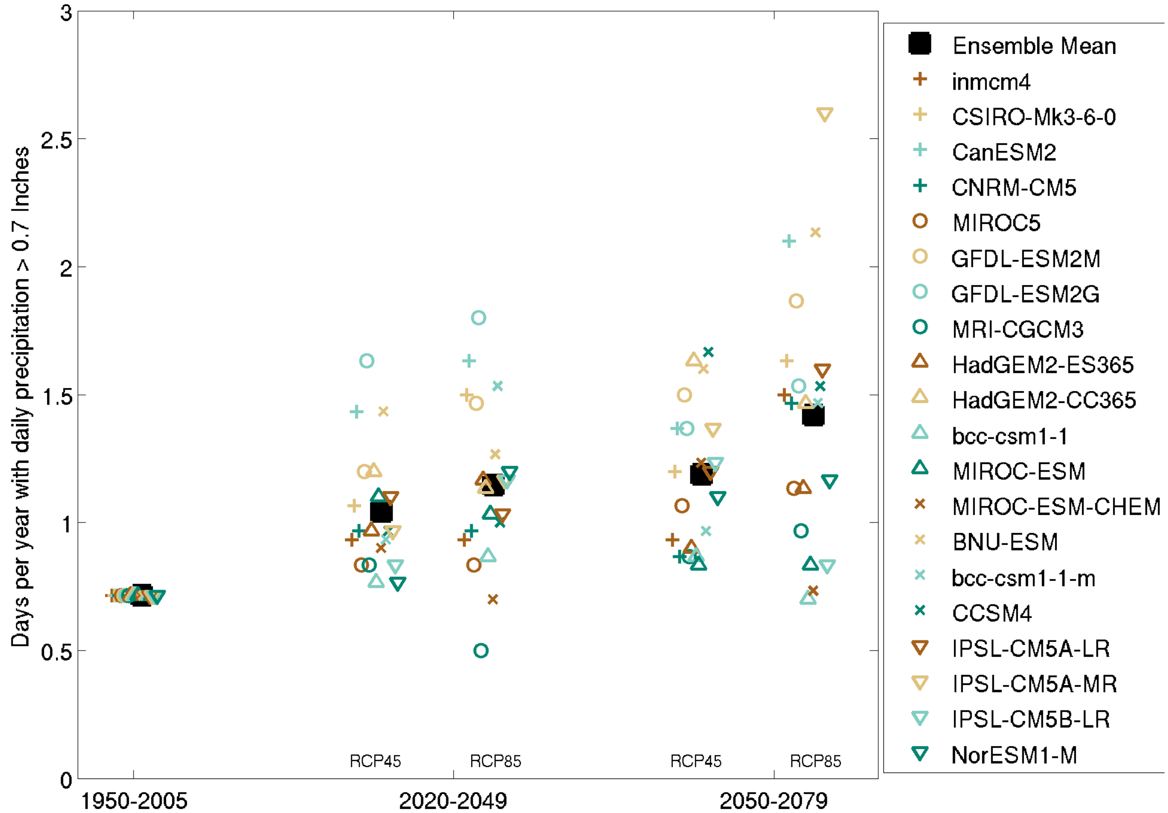

Figure 2.1: Modeled average number of heavy precipitation events (daily precipitation exceeding 0.7 inches) per year under historical (left), early 21st century (middle) and mid-21st century (right) from 20 downscaled climate models for low emissions (RCP4.5) and high emissions (RCP8.5) scenarios. The black box shows the average of the 20 models.

Table 2.1: Average number of heavy precipitation days (daily precipitation >0.7 inches) per year for different models (rows) and time period/scenarios (columns).

	1950-2005	2020-2049 RCP45	2020-2049 RCP85	2050-2079 RCP45	2050-2079 RCP45
inmcm4	0.7	0.9	0.9	0.9	1.5
CSIRO-Mk3-6-0	0.7	1.1	1.5	1.2	1.6
CanESM2	0.7	1.4	1.6	1.4	2.1
CNRM-CM5	0.7	1.0	1.0	0.9	1.5
MIROC5	0.7	0.8	0.8	1.1	1.1
GFDL-ESM2M	0.7	1.2	1.5	1.5	1.9
GFDL-ESM2G	0.7	1.6	1.8	1.4	1.5
MRI-CGCM3	0.7	0.8	0.5	0.9	1.0
HadGEM2-ES365	0.7	1.0	1.2	0.9	1.1
HadGEM2-CC365	0.7	1.2	1.1	1.6	1.5
bcc-csm1-1	0.7	0.8	0.9	0.9	0.7
MIROC-ESM	0.7	1.1	1.0	0.8	0.8
MIROC-ESM-CHEM	0.7	0.9	0.7	1.2	0.7
BNU-ESM	0.7	1.4	1.3	1.6	2.1
bcc-csm1-1-m	0.7	0.9	1.5	1.0	1.5
CCSM4	0.7	1.0	1.0	1.7	1.5
IPSL-CM5A-LR	0.7	1.1	1.0	1.2	1.6
IPSL-CM5A-MR	0.7	1.0	1.2	1.4	2.6
IPSL-CM5B-LR	0.7	0.8	1.2	1.2	0.8
NorESM1-M	0.7	0.8	1.2	1.1	1.2
MEAN	**0.7**	**1.0**	**1.1**	**1.2**	**1.4**

References

Abatzoglou, J.T., and T.J. Brown. 2012, A Comparison of Statistical Downscaling Methods Suited for Wildfire Applications, International Journal of Climatology, doi:10.1002/joc.2312

Abatzoglou, J.T., 2013, Development of gridded surface meteorological data for ecological applications and modeling, International Journal of Climatology, doi: 10.1002/joc.3413

Metric III: Irrigation demand

Defined: Evapotranspiration is the water lost through evaporation and transpiration from vegetation. To keep both crops and urban landscapes "well watered" during periods where precipitation does not meet the water demands of vegetation, additional water is required through irrigation.

How it is calculated: Reference evapotranspiration (ETo) is the potential amount of water used by a reference grass surface for given ambient meteorological conditions. ETo is calculated using the Penman-Monteith equation, which is the standard for estimating crop water use in Idaho when meteorological observations are complete (Allen et al., 1998). Actual evapotranspiration can differ from ETo as a function of both vegetation type and if vegetation undergoes water stress. For the purposes of this exercise, ETo will be used as it approximates the amount of water a reference grass surface will use when it is well watered. The total ETo from April through October is used to approximate the irrigation demand. Although precipitation does occur during this time period, it is typically insufficient to meet ETo demands.

Data: Monthly temperature, wind speed, solar radiation and humidity data were obtained from 20 downscaled climate models (Table 3.1) for a ~2.5 mile by 2.5 mile grid point centered over Boise, Idaho (43.61°N, 116.2°W). These data were downscaled using the Multivariate Adaptive Constructed Analogs (MACA, Abatzoglou and Brown, 2012) statistical downscaling method that applies observational relationships between fine-scale and coarse resolution meteorology to the coarse resolution output of global climate models. The gridded observational dataset of Abatzoglou (2013) from 1979-2016 was used as the training data. These data are not intended to provide fine-scale information on climate at the scales of individual buildings, parks, or neighborhoods -- all of which have their own microclimate, but rather a broader scale representation of climate experienced throughout the Boise metropolitan area. An additional factor is further included to account for the fact that under elevated carbon dioxide concentrations, crops before more water efficient by closing their stomata and limiting transpiration rates. There are numerous ways to approximate this effect, and science is still evolving on precisely how climate change and additional carbon dioxide will alter water use by crops. For the purposes of this analysis, an empirical transformation of Kruijt et al. (2008) is applied for a grass surface that effectively reduces ETo with rising levels of carbon dioxide. A scalar factor is applied to each year by considering the projected changes in atmospheric carbon dioxide levels under low and high emission scenarios from a reference 1980 baseline. This has the effect of approximately reducing the calculated ETo for low and high emissions scenarios by 1.5% and 1.8%, respectively, for the early 21st century (2020-2049), and 2.25% and 3.65% for the mid 21st century (2050-2079).

Analysis: The total ETo during irrigation season (April-October) was calculated for the historical modeled data (1950-2005) and future climate scenarios for the early (2020-2049) and mid-21st century (2050-2079).

Results: The annual April-October ETo over the contemporary climate was 41.4 inches, which is comparable (about 3% higher) with that of the Boise AgriMet station. Despite the enhanced water use efficiency of crops with enhanced carbon dioxide concentrations, estimated ETo is projected to increase by approximately 2 inches (5%) by the early-21st century, and an average of 2.6 inches (+6.4%) and 4 inches (+9.7%) by the mid-21st century. These increases are based on substantial warming of summer temperatures, increased vapor pressure deficit (difference between atmospheric moisture and potential water holding capacity of the air), and slight increases in solar radiation (a function of more clear days). For the mid-21st century under high-emissions, a couple models project increase in ETo of 6 or more inches (14.5%), whereas a couple project more subtle increases of around 2 inches.

Summary: Human-caused climate change will increase evaporative demand and hence irrigation demand during the warm season across Boise. An increase of approximately 2 inches of irrigation is projected by the early 21st century and up to 4 inches of irrigation by the mid-21st century under high emissions scenario.

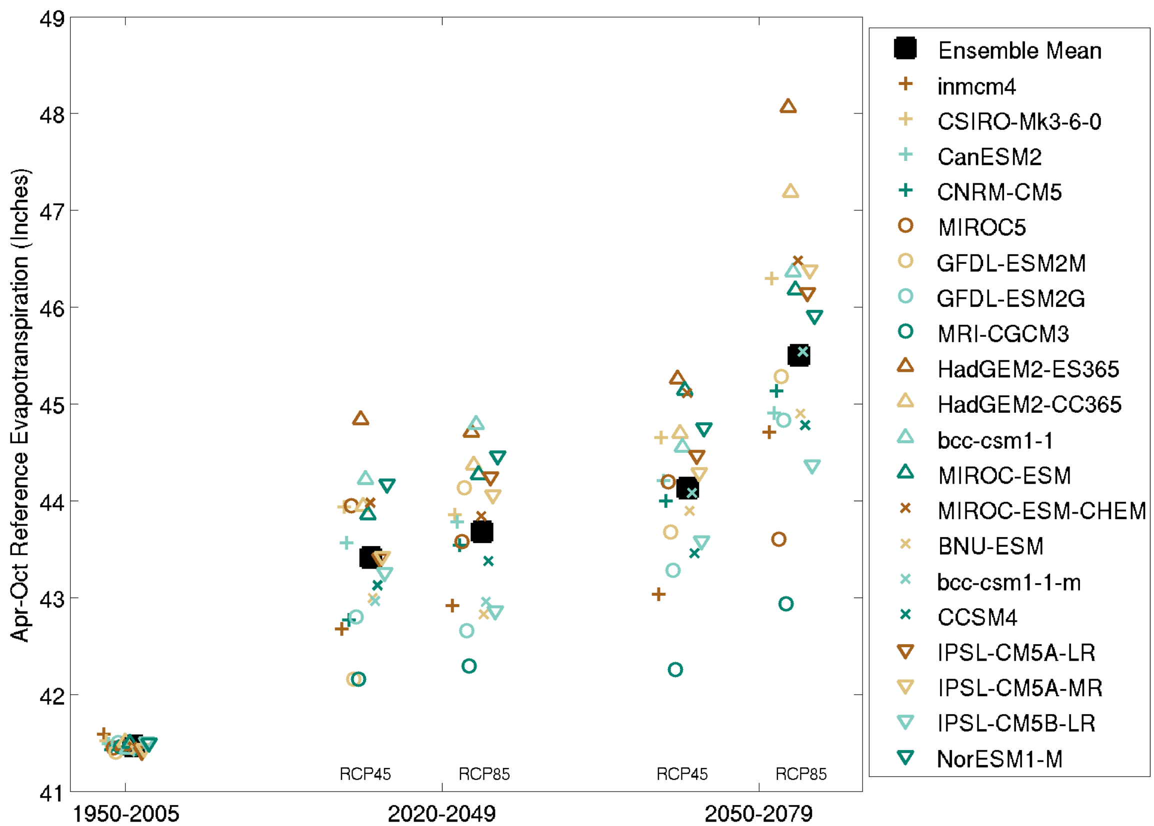

Figure 3.1: Modeled average reference evapotranspiration (ETo) from April-October under historical (left), early 21st century (middle) and mid-21st century (right) from 20 downscaled climate models for low emissions (RCP4.5) and high emissions (RCP8.5) scenarios. The black box shows the average of the 20 models.

Table 3.1: Average reference evapotranspiration (inches) from April-October for different models (rows) and time period/scenarios (columns).

	1950-2005	2020-2049 RCP45	2020-2049 RCP85	2050-2079 RCP45	2050-2079 RCP45
inmcm4	41.6	42.7	43.0	43.1	44.8
CSIRO-Mk3-6-0	41.6	44.0	43.9	44.7	46.3
CanESM2	41.5	43.6	43.8	44.3	45.0
CNRM-CM5	41.5	42.8	43.6	44.0	45.2
MIROC5	41.5	44.0	43.6	44.2	43.7
GFDL-ESM2M	41.5	42.2	44.2	43.7	45.3
GFDL-ESM2G	41.6	42.9	42.7	43.3	44.9
MRI-CGCM3	41.5	42.2	42.3	42.3	43.0
HadGEM2-ES365	41.5	44.9	44.8	45.3	48.1
HadGEM2-CC365	41.6	44.0	44.4	44.7	47.2
bcc-csm1-1	41.5	44.3	44.8	44.6	46.4
MIROC-ESM	41.5	43.9	44.3	45.2	46.2
MIROC-ESM-CHEM	41.5	44.0	43.9	45.2	46.5
BNU-ESM	41.5	43.0	42.9	43.9	45.0
bcc-csm1-1-m	41.5	43.0	43.0	44.1	45.6
CCSM4	41.5	43.2	43.4	43.5	44.8
IPSL-CM5A-LR	41.5	43.5	44.3	44.5	46.2
IPSL-CM5A-MR	41.5	43.5	44.1	44.3	46.4
IPSL-CM5B-LR	41.6	43.3	42.9	43.6	44.4
NorESM1-M	41.5	44.2	44.5	44.8	46.0
MEAN	**41.5**	**43.5**	**43.7**	**44.2**	**45.6**

References

Abatzoglou, J.T., and T.J. Brown. 2012, A Comparison of Statistical Downscaling Methods Suited for Wildfire Applications, International Journal of Climatology, doi:10.1002/joc.2312

Abatzoglou, J.T., 2013, Development of gridded surface meteorological data for ecological applications and modeling, International Journal of Climatology, doi: 10.1002/joc.3413

Allen, R.G., Pereira, L.S., Raes, D. and Smith, M., 1998. Crop evapotranspiration-Guidelines for computing crop water requirements-FAO Irrigation and drainage paper 56. *FAO, Rome*, *300*(9), p. D05109.

Kruijt, B., Witte, J.P.M., Jacobs, C.M. and Kroon, T., 2008. Effects of rising atmospheric CO 2 on evapotranspiration and soil moisture: a practical approach for the Netherlands. *Journal of Hydrology*, *349*(3), pp.257-267.

Metric IV: Summer drought

Defined: Drought is defined by the relative water demand exceeding the relative water supply. Whereas water demand can relate to a number of factors external to climate processes, variability in potential evapotranspiration (ETo) plays a first order role in determining water demand by vegetation and crops. The supply of water is primarily associated with precipitation and precipitation timing. Collectively, a set of drought indices are routinely used by the United States Drought Monitor and Idaho Department of Water Resources to track drought and establish drought declarations. At the forefront of these indices is the Palmer Drought Severity Index, or PDSI.

How it is calculated: PDSI is calculated following the procedures outlined by Palmer (1965). The PDSI uses a simplified monthly water budget and considers water supply (precipitation), water demand (ETo) and runoff. The PDSI does not track snowfall and treats all precipitation as liquid. PDSI was designed to track soil moisture in agricultural systems, but has been shown to correspond well with annual streamflow variability, wildfire activity and other drought related impacts in the interior western US including Idaho. The PDSI is an index, where negative values indicate drier than normal, positive values wetter than normal. Nominally, thresholds of PDSI are used to identify drought. For our purposes we consider moderate drought as PDSI<-2 and exceptional drought as PDSI<-4. Historically, moderate drought occurs about 25% of the time, whereas exceptional drought occurs around 8% of the time in the greater Boise area according to these measures. While PDSI is calculated each month, we synthesize results by only looking at summer (June-August) PDSI.

Data: Monthly precipitation and ETo were calculated from 20 downscaled climate models (Table 4.1) for a ~2.5 mile by 2.5 mile grid point centered over Boise, Idaho (43.61°N, 116.2°W). These data were downscaled using the Multivariate Adaptive Constructed Analogs (MACA, Abatzoglou and Brown, 2012) statistical downscaling method that applies observational relationships between fine-scale and coarse resolution meteorology to the coarse resolution output of global climate models. The gridded observational dataset of Abatzoglou (2013) from 1979-2016 was used as the training data. These data are not intended to provide fine-scale information on climate at the scales of individual buildings, parks, or neighborhoods -- all of which have their own microclimate, but rather a broader scale representation of climate experienced throughout the Boise metropolitan area. We apply the same correction for estimating curtailments in ETo under elevated carbon dioxide concentrations as outlined in the preceding metric. The PDSI calculation also requires an estimate of surface available water holding capacity given its goal in simulating soil moisture variability. Nominally, we assigned this to 150mm, which is the average value given for national analysis.

Analysis: The odds of moderate (PDSI<-2) and exceptional (PDSI<-4) was examined separately for each of the 20 downscaled climate models for the historical modeled data (1950-2005) and future climate scenarios for the early (2020-2049) and mid-21st century (2050-2079).

Results: The estimated percent of summers with at least moderate (PDSI<-2) and at least exceptional drought (PDSI<-4) over the historical climate experiments (1950-2005) was 26.5% and 8.5%, respectively. Most models project an increase in drought frequency by the early-21st century and slight additional increase by the mid-21st century (Table 4.1). A total of 3-5 models did not show a significant increase. The multi-model mean suggests that 45% and 52% of summers are projected to experience at least moderate drought by the mid-21st century under low and high emission scenarios, respectively, compared to 26.5% under baseline climatic conditions. The frequency of exceptional drought is projected to increase by 100-200% under future climate projections by the mid-21st century (Table 4.2). These changes are a direct response to increases in ETo (outlined in the preceding section).

Summary: Human-caused climate change will increase the frequency of moderate to exceptional summer drought across Boise. Moderate drought which currently occurs in around 1 of every 4 years, on average, is projected to occur in 1 of every 2 years, on average, by the mid-21st century. Likewise, exceptional drought that historically occurs on average in 1 of every 12 years, is projected to occur in nearly 1 of every 3 to 4 years by the mid-21st century.

Table 4.1: Percent of summers with moderate drought (June-August PDSI less than -2).

	1950-2005	2020-2049 RCP45	2020-2049 RCP85	2050-2079 RCP45	2050-2079 RCP45
inmcm4	34	40	43	30	37
CSIRO-Mk3-6-0	30	63	53	30	67
CanESM2	23	30	43	43	40
CNRM-CM5	27	27	47	40	57
MIROC5	27	67	57	57	57
GFDL-ESM2M	23	30	23	37	20
GFDL-ESM2G	32	30	40	17	43
MRI-CGCM3	20	27	23	37	23
HadGEM2-ES365	25	47	43	47	73
HadGEM2-CC365	23	30	33	33	50
bcc-csm1-1	23	50	57	57	60
MIROC-ESM	29	47	67	57	83
MIROC-ESM-CHEM	27	60	73	37	87
BNU-ESM	32	33	27	47	53
bcc-csm1-1-m	29	27	53	33	57
CCSM4	30	43	30	40	37
IPSL-CM5A-LR	23	50	60	63	53
IPSL-CM5A-MR	29	47	40	40	53
IPSL-CM5B-LR	27	47	50	40	57
NorESM1-M	21	57	47	40	43
MEAN	**26.7**	**42.6**	**45.5**	**41.3**	**52.5**

Table 4.2: Percent of summers with moderate drought (June-August PDSI less than -4).

	1950-2005	2020-2049 RCP45	2020-2049 RCP85	2050-2079 RCP45	2050-2079 RCP45
inmcm4	9	10	27	10	23
CSIRO-Mk3-6-0	9	27	27	10	27
CanESM2	9	23	17	23	17
CNRM-CM5	7	20	23	23	20
MIROC5	7	43	27	33	47
GFDL-ESM2M	7	13	10	13	3
GFDL-ESM2G	11	17	23	0	27
MRI-CGCM3	5	10	10	13	10
HadGEM2-ES365	11	23	27	10	37
HadGEM2-CC365	7	20	10	17	30
bcc-csm1-1	9	10	17	27	37
MIROC-ESM	9	23	50	23	60
MIROC-ESM-CHEM	11	23	47	23	60
BNU-ESM	7	17	7	27	37
bcc-csm1-1-m	11	7	23	17	27
CCSM4	14	23	20	17	13
IPSL-CM5A-LR	7	17	40	20	30
IPSL-CM5A-MR	11	23	17	20	27
IPSL-CM5B-LR	5	13	20	23	30
NorESM1-M	4	27	27	20	20
MEAN	**8.5**	**19.5**	**23.5**	**18.5**	**29.1**

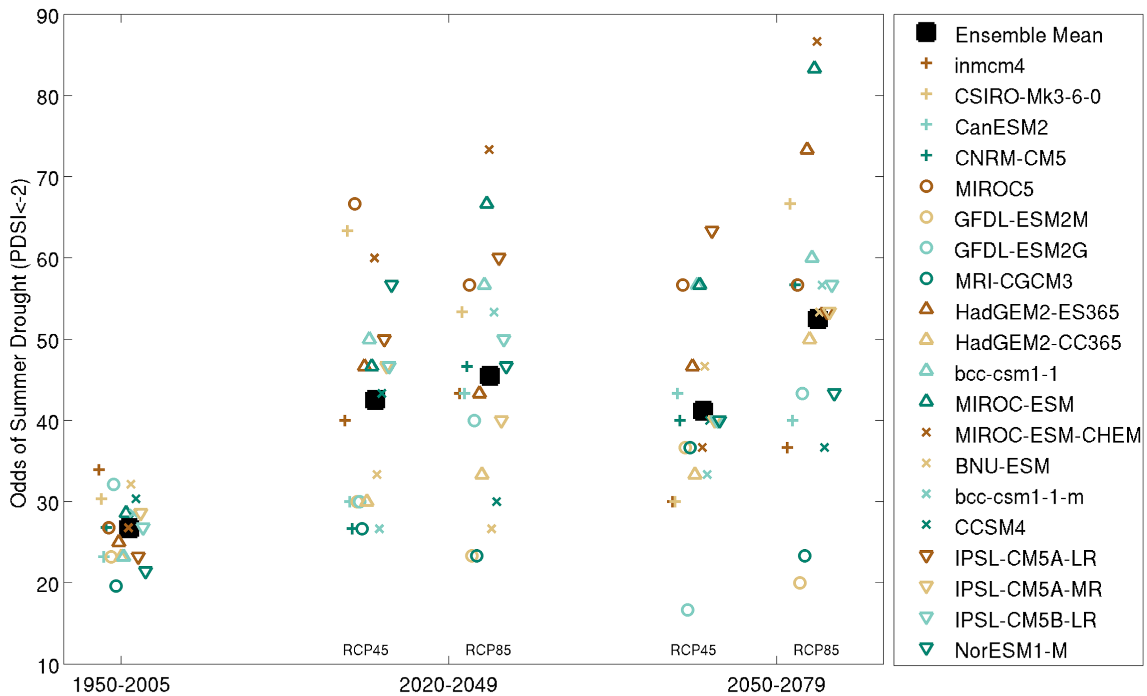

Figure 4.1: Modeled probability of moderate summer drought (PDSI<-2) under historical (left), early 21st century (middle) and mid-21st century (right) from 20 downscaled climate models for low emissions (RCP4.5) and high emissions (RCP8.5) scenarios. The black box shows the average of the 20 models.

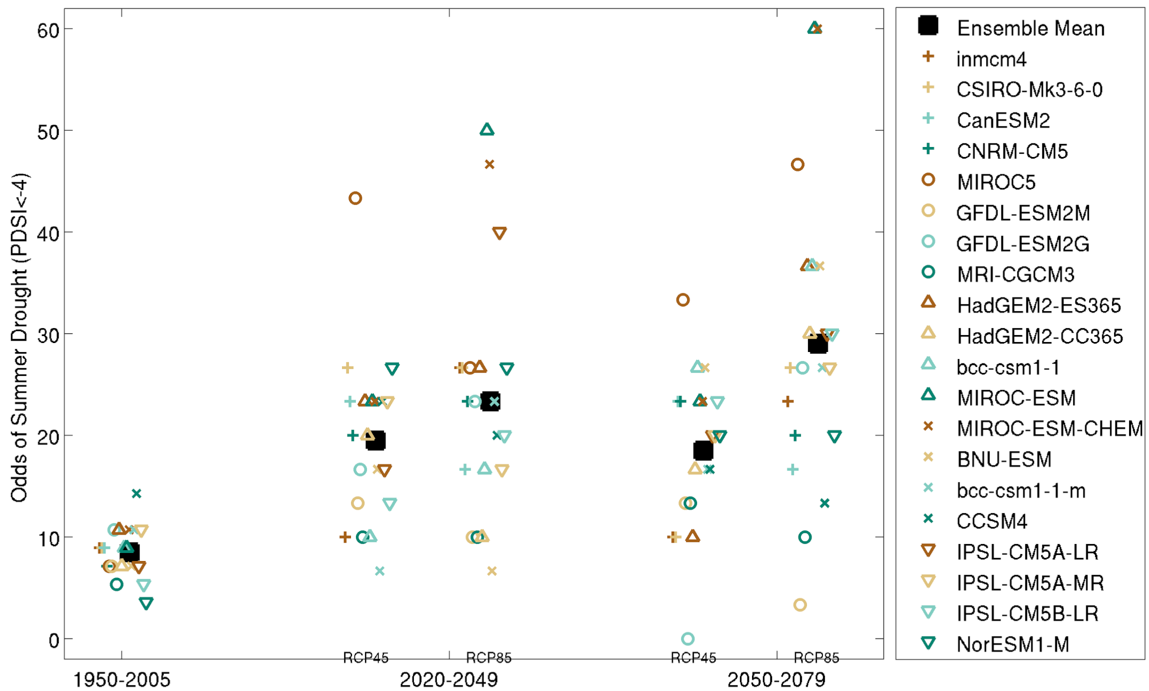

Figure 4.2: Modeled probability of exceptional summer drought (PDSI<-4) under historical (left), early 21st century (middle) and mid-21st century (right) from 20 downscaled climate models for low emissions (RCP4.5) and high emissions (RCP8.5) scenarios. The black box shows the average of the 20 models.

References

Abatzoglou, J.T., and T.J. Brown. 2012, A Comparison of Statistical Downscaling Methods Suited for Wildfire Applications, International Journal of Climatology, doi:10.1002/joc.2312

Abatzoglou, J.T., 2013, Development of gridded surface meteorological data for ecological applications and modeling, International Journal of Climatology, doi: 10.1002/joc.3413

Palmer, W.C., 1965. Meteorological drought (Vol. 30). Washington, DC: US Department of Commerce, Weather Bureau.

Metric V: Wildfire danger and smoke potential

Defined: Wildfire potential consider multiple factors including ignitions, winds, fuel abundance and fuel dryness. Fire-regimes vary substantially between the rangeland systems of southern Idaho and the adjacent forested systems along the Boise front range. Forested systems have more direct links to climate variability as fuel moisture typically limits large wildfire potential in these systems. Conversely, the abundance of fuels in semi-arid rangelands often limits large fire potential. Nonetheless, the occurrence of very large fires and total burned area in both ecosystems exhibits links to fuel dryness during the fire season (e.g., Abatzoglou and Kolden, 2013; Riley et al., 2013). Climate change may alter the probability of wind events, lightning occurrence and other factors important to wildfire potential. However, the primarily means through which climate change is expected to impact wildfire potential is through fuel dryness.

How it is calculated: There are several approaches for estimating fuel aridity and dryness. We use the 1000-hour dead fuel moisture from the National Fire Danger Rating System as the metric of choice here given its use in wildland fire management in the region and intuitive nature. 1000-hour fuels represent dead and downed branches with diameters between 3-8”, typical of forested regions surrounding Boise that are responsible for long-lived wildfire events (e.g., Pioneer Fire of 2016) that can burn for weeks to months at a time and are responsible for chronic smoke potential for the greater Boise metropolitan area. The probability of large fires has been shown to be well related to these indices (e.g., Riley et al., 2013; Freeborn et al., 2015) and hence we consider high risk days as those where the 1000-hour dead fuel moisture is below the historical 5th percentile. This nominally results in a baseline of about 18 days per year of high risk for large fire potential based strictly on fuel dryness.

Data: Daily temperature, relative humidity, precipitation, and solar radiation were obtained from 18 downscaled climate models (Table 5.1) for a ~2.5 mile by 2.5 mile grid point centered over Boise, Idaho (43.61°N, 116.2°W). Two of the 20 models previously considered did not have relative humidity data. These data were downscaled using the Multivariate Adaptive Constructed Analogs (MACA, Abatzoglou and Brown, 2012) statistical downscaling method that applies observational relationships between fine-scale and coarse resolution meteorology to the coarse resolution output of global climate models. The gridded observational dataset of Abatzoglou (2013) from 1979-2016 was used as the training data. These data are not intended to provide fine-scale information on climate at the scales of individual buildings, parks, or neighborhoods -- all of which have their own microclimate, but rather a broader scale representation of climate experienced throughout the Boise metropolitan area and nearby forested systems.

Analysis: The number of high risk days for large fire potential defined by 1000-hour fuel moisture below the 5th percentile level was examined separately for each of the 18 downscaled climate models for the historical modeled data (1950-2005) and future climate scenarios for the early (2020-2049) and mid-21st century (2050-2079).

Results: Most all models show an increase in the number of days per year with high fire danger by the early and mid 21st century (Figure 5.1). By the early 21st century an additional 8 days (+44%) of year of high fire danger is projected compared to a historical baseline of 18 days per year, with 12-18 additional days (+66-100%) of high fire danger by the mid-21st century under low and high emission scenarios, respectively. All but one model (MIROC5) shows at least a 7 day increase in the number of days per year of high fire danger under high emissions scenario for the mid-21st century, with a couple models projecting an additional 30+ days per year.

Supplemental Analysis: To approximate the potential for very large fires within the Boise airshed under climate change scenarios we consider the results of Barbero et al., (2015) who modeled very large fire potential (fires that burned at least 12,500 acres) under mid-21st century climatic conditions for the high emission scenario using 17 of the 18 models mentioned here (Figue 5.2). Barbero et al. (2015) developed separate models for different ecotypes (e.g., forests versus rangelands) on ~40 mile x ~40 mile grids across the US using a number of climate variables that exhibited strong relationships to observed very large fires. We consider the probability of very large fires within a 120 mile radius of Boise (Boise airshed) as having air quality impacts on the metropolitan area. This radius captures a majority of the fire related smoke impacts on Boise (Idaho Department of Environmental Quality), although longer distance smoke transport can occur. Historical experiments under a contemporary climate project an average of 2 very large fires per year within the Boise airshed. Climate change scenarios for the 2041-2070 period under high emission scenarios project a significant increase with an average of 7.8 very large fires per year (+290% increase) within the region, although the results vary from model to model (Table 5.2).

Summary: Human-caused climate change will increase conditions conducive to regionally large fire seasons and very large fires by increasing fuel dryness during the fire season. The duration of the summer period under which fuels are projected to be critically dry is projected to increase 40-100% under the climate scenarios considered. Whereas a couple models show nominal change, a vast majority of models showed substantial increases. Furthermore, a regional modeling effort suggest that the odds of very large fires in the Boise airshed region will increase by nearly 300% by the mid-21st century under high emission scenarios, increasing the potential for chronic air quality problems within the metropolitan area. A significant caveat to these results are impending changes in fuel management or the negative feedbacks of fires, both which can reduce fuel loads and limit projected increases in wildfire and smoke impacts.

Table 5.1: Average number of days per year with very low 1000-hour fuel moisture (below the historical 5th percentile).

	1950-2005	2020-2049 RCP45	2020-2049 RCP85	2050-2079 RCP45	2050-2079 RCP45
inmcm4	18.0	37.3	44.9	45.8	65.4
CSIRO-Mk3-6-0	16.6	37.8	36.1	37.7	50.0
CanESM2	15.2	23.5	26.2	29.8	22.7
CNRM-CM5	19.1	28.8	37.9	34.9	40.4
MIROC5	15.0	22.4	21.0	18.8	6.5
GFDL-ESM2M	15.7	19.2	29.1	34.6	35.2
GFDL-ESM2G	14.0	18.6	18.2	10.1	22.6
MRI-CGCM3	18.8	19.0	23.5	23.6	27.3
HadGEM2-ES365	22.7	37.0	34.3	30.4	47.6
HadGEM2-CC365	23.5	21.4	29.6	23.2	40.8
bcc-csm1-1	23.8	35.7	39.0	32.5	45.9
MIROC-ESM	18.7	19.7	30.1	15.7	35.3
MIROC-ESM-CHEM	19.2	23.1	39.2	17.6	51.2
BNU-ESM	17.5	21.3	22.1	23.7	27.4
bcc-csm1-1-m	18.0	28.0	26.0	21.5	30.4
IPSL-CM5A-LR	21.8	25.8	38.7	33.1	43.9
IPSL-CM5A-MR	16.9	21.9	30.1	24.7	34.6
IPSL-CM5B-LR	21.5	28.8	25.0	21.6	34.2
MEAN	**18.7**	**26.1**	**30.6**	**26.6**	**36.8**

Table 5.2: Average number of very large wildfires (>12,500 acres) per year within 120 miles of Boise as modeled by Barbero et al., (2015b).

	1971-2000	2041-2070 RCP85
inmcm4	2.0	10.3
CSIRO-Mk3-6-0	1.9	9.4
CanESM2	1.9	7.8
CNRM-CM5	2.1	8.6
MIROC5	2.0	4.3
GFDL-ESM2M	2.0	8.0
GFDL-ESM2G	2.0	5.3
MRI-CGCM3	2.0	4.4
HadGEM2-ES365	2.0	10.2
HadGEM2-CC365	1.9	10.0
bcc-csm1-1	2.2	6.5
MIROC-ESM	2.0	9.5
MIROC-ESM-CHEM	2.2	12.6
BNU-ESM	2.0	6.4
bcc-csm1-1-m	2.1	6.6
IPSL-CM5A-LR	2.0	9.0
IPSL-CM5B-LR	2.1	5.4
MEAN	**2.0**	**7.9**

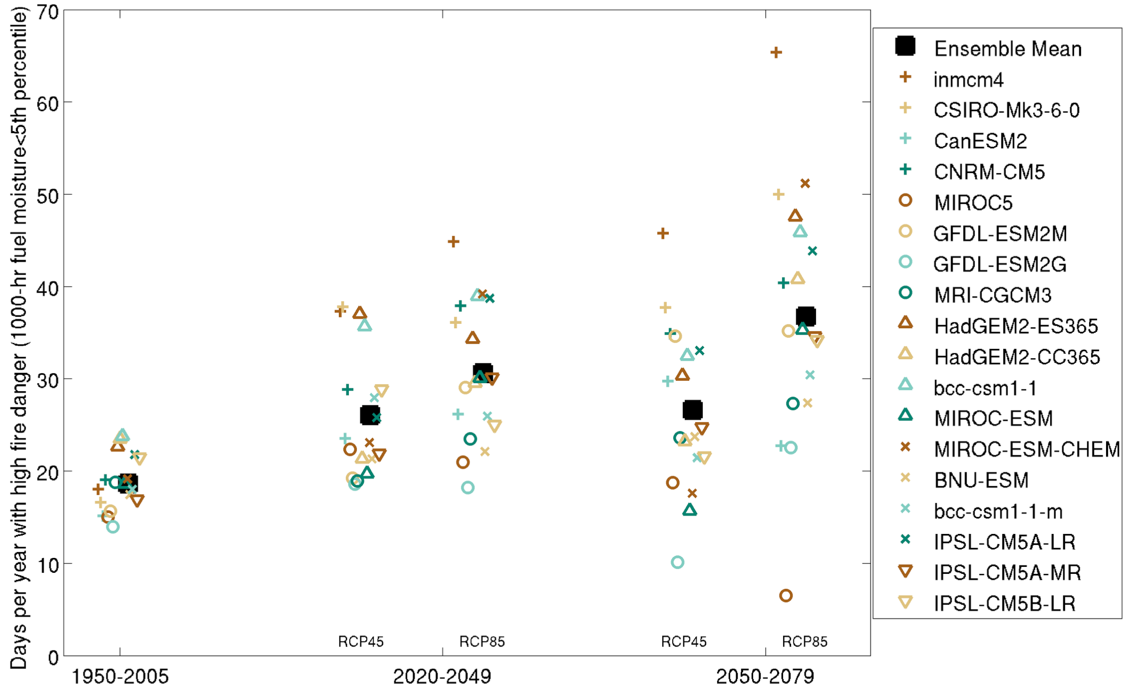

Figure 5.1: Modeled probability of high fire danger (1000-hour dead fuel moisture below the historical 5th percentile) under historical (left), early 21st century (middle) and mid-21st century (right) from 20 downscaled climate models for low emissions (RCP4.5) and high emissions (RCP8.5) scenarios. The black box shows the average of the 20 models.

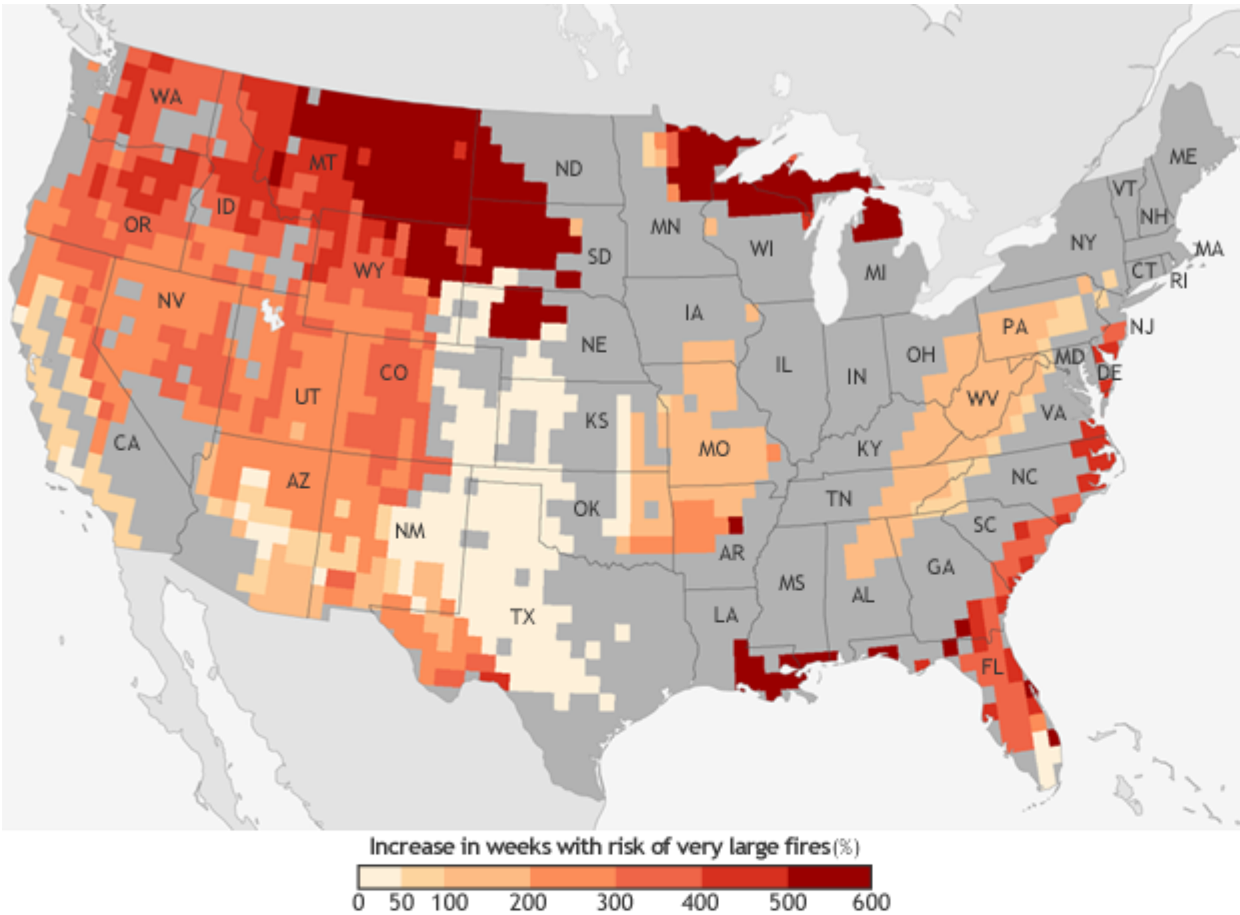

Figure 5.2: Projected changes in the probability of very large wildfires across the continental US by the mid-21st century (2041-2070) under high emission scenario. Results show the multi-model mean change. Note the 3-4 fold increase near Boise. Figure from NOAA [https://www.climate.gov/news-features/featured-images/risk-very-large-fires-could-increase-sixfold-mid-century-us].

References

Abatzoglou J.T., Kolden C.A. (2013) Relationships between climate and macroscale area burned in the western United States. *International Journal of Wildland Fire* **22**, 1003–1020.

Abatzoglou, J.T., and T.J. Brown. 2012, A Comparison of Statistical Downscaling Methods Suited for Wildfire Applications, International Journal of Climatology, doi:10.1002/joc.2312

Abatzoglou, J.T., 2013, Development of gridded surface meteorological data for ecological applications and modeling, International Journal of Climatology, doi: 10.1002/joc.3413

Barbero, R.; Abatzoglou, J.T.; Larkin, N.K.; Kolden, C.A.; Stocks, B. 2015. Climate change presents increased potential for very large fires in the contiguous United States. International Journal of Wildland Fire. *International Journal of Wildland Fire* **24**, 892–899.

Freeborn, P.H., Cochrane, M.A. and Jolly, W.M., 2015. Relationships between fire danger and the daily number and daily growth of active incidents burning in the northern Rocky Mountains, USA. *International Journal of Wildland Fire*, *24*(7), pp.900-910.

Riley K.L., Abatzoglou J.T., Grenfell I.C., Klene A.E., Heinsch F.A. 2013. The relationship of large fire occurrence with drought and fire danger indices in the western USA, 1984–2008: the role of temporal scale. *International Journal of Wildland Fire* **22**, 894

Metric VI: Seasonal Streamflow

Defined: Streamflow represents the volume of water passing through a river or stream, often measured in cubic feet per second, that is also a proxy for river heights. Streamflow is an integrated measure of surface water availability as the volume and timing incorporate precipitation amount, precipitation phase and snowpack storage, and evapotranspiration from vegetation and soils. Processes such as water withdrawals and diversions can substantially alter streamflow. Natural flow refers to the natural runoff of a watershed or waterbody that would have occurred in the absence of human influences on the watershed. While the Boise River is heavily managed, we use naturalized flow as it more purely captured the influence of environmental change on water levels. Numerical values thus should not be directly compared with observed flow on the system. However, we emphasize that relative differences between baseline and future climate conditions should provide a measure of potential changes.

How it is calculated: Hydrologic models are used to simulate surface water dynamics including snowpack, soil moisture and runoff. The Variable Infiltration Capacity (VIC, Liang et al., 1994) model was used in this analysis given its widespread usage in climate-hydrology studies across the western US both operationally and for climate studies. The VIC model was done by the University of Washington as part of the USGS Northwest Climate Science Center funded Integrated Scenarios of the Future Environment project. These models used 10 of the aforementioned 20 downscaled climate scenarios, and model processes including precipitation phase, snowmelt, and soil-vegetation interactions (Table 6.1). A river routing scheme (Lohmann et al., 1998) was used to connect runoff from the upstream watershed to simulate river flow at various locations.

Data: Daily streamflow was obtained from 10 climate projections for a location on the Boise River upstream of Boise near Lucky Peak Inflow. These data are for naturalized flow and do not account for upstream diversions, dam operations, etc. Given that the Boise River is heavily managed, it is not recommended to focus on the actual numbers, but rather differences between the scenarios and the historical baseline.

Analysis: Monthly average streamflow was examined separately for each of the 10 downscaled climate models for the historical modeled data (1950-2005) and future climate scenarios for the early (2020-2049) and mid-21st century (2050-2079). We also considered changes in annual mean streamflow as a proxy for examining changes in total water availability.

Results: Models show a seasonal shift in streamflow, with more runoff in winter and spring and less during the summer months (Figure 6.1). This is a response to decreased mountain snowpack in the upstream watershed and increase in the amount of precipitation falling as rain and running off earlier in the year. A substantial reduction in flow is modeled for July across all models (Figure 6.2, Table 6.1) with an average 50% decrease by the early 21st century under the low emissions scenario, and an average 70% decrease by the mid-21st century under the high emission scenario. The annual mean flow shows inconsistent changes across models and scenarios (Figure 6.3, Table 6.2) with increases and decreases as simulated by the 10 models.

Summary: Human-caused climate change will shift the timing of river levels across the broader region including the Boise River leading to more runoff in the winter and spring and less during the summer months. Conversely, the total flow is not projected to change significantly with a lot of variability simulated across models.

Table 6.1: Monthly mean streamflow (cubic feet per second) as simulated by the Variable Infiltration Capacity model for the Boise River near Lucky Peak for different climate models and time periods. Model output is for unregulated river, hence should be different than observed data.

	1950-2005	2020-2049 RCP45	2020-2049 RCP85	2050-2079 RCP45	2050-2079 RCP45
bcc-csm1-1-m	1964	1856	1753	2172	1922
NorESM1-M	1983	1695	1985	2119	1981
MIROC5	1983	1621	1758	1847	1831
IPSL-CM5A-MR	1963	1979	1903	1954	2114
HadGEM2-ES365	1994	1721	1920	2029	1684
HadGEM2-CC365	1999	2191	2278	2195	1963
CSIRO-Mk3-6-0	1977	1711	1800	1756	1788
CNRM-CM5	1978	2101	1955	2069	1846
CanESM2	2016	1983	2073	2069	2252
CCSM4	1984	2025	1904	1997	1960
MEAN	**1984**	**1888 (-5%)**	**1933 (-3%)**	**2021 (+2%)**	**1934 (-3%)**

Table 6.2: July mean streamflow (cubic feet per second) as simulated by the Variable Infiltration Capacity model for the Boise River near Lucky Peak for different climate models and time periods. Model output is for unregulated river, hence should be different than observed data.

	1950-2005	2020-2049 RCP45	2020-2049 RCP85	2050-2079 RCP45	2050-2079 RCP45
bcc-csm1-1-m	2879	1796	1302	1698	974
NorESM1-M	2958	1118	1110	1642	931
MIROC5	3741	1178	838	1336	806
IPSL-CM5A-MR	3244	1863	1002	1233	820
HadGEM2-ES365	3141	1424	940	1418	718
HadGEM2-CC365	3077	1835	1495	2005	761
CSIRO-Mk3-6-0	3243	1205	1029	1204	899
CNRM-CM5	3534	2350	1475	2079	1067
CanESM2	3201	1141	868	1128	852
CCSM4	3411	1486	1288	1081	941
MEAN	**3242**	**1540 (-53%)**	**1135 (-65%)**	**1482 (-54%)**	**877 (-73%)**

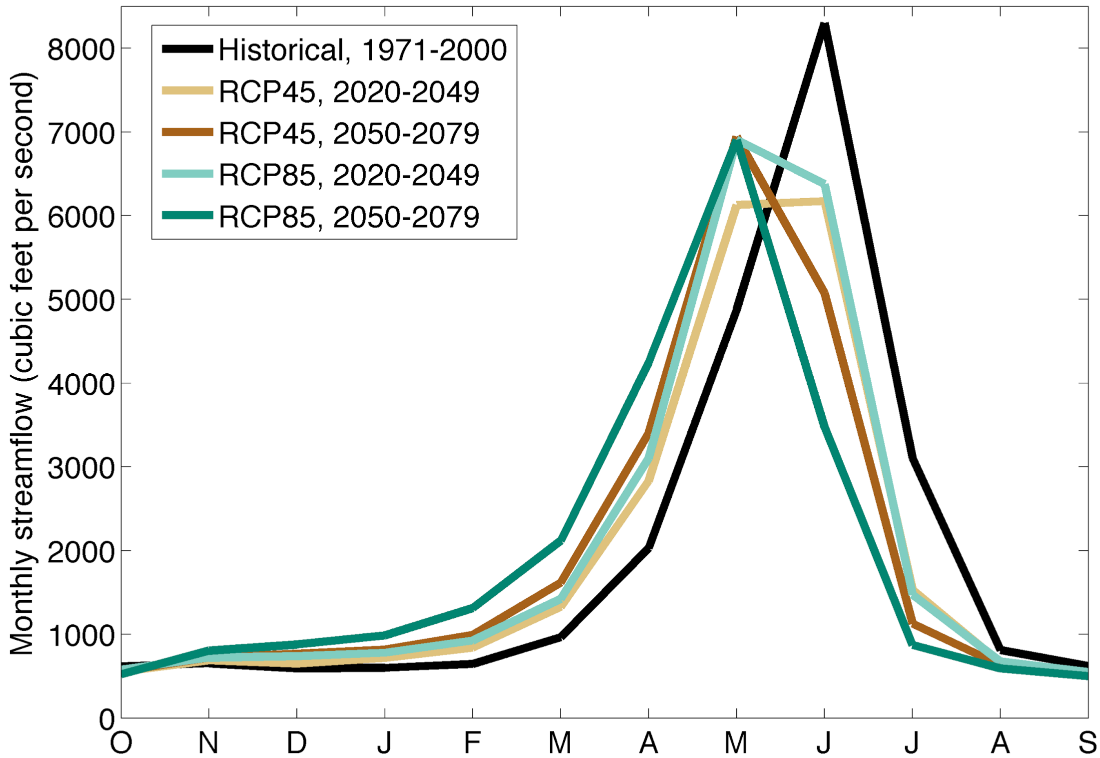

Figure 6.1: Monthly mean streamflow in cubic feet per second for the Boise River near Lucky Peak averaged over 10 climate models for historical (black), early 21st century under low emissions (beige), mid 21st century under low emissions (brown), early 21st century under high emissions (light green) and mid-21st century under high emissions (dark green).

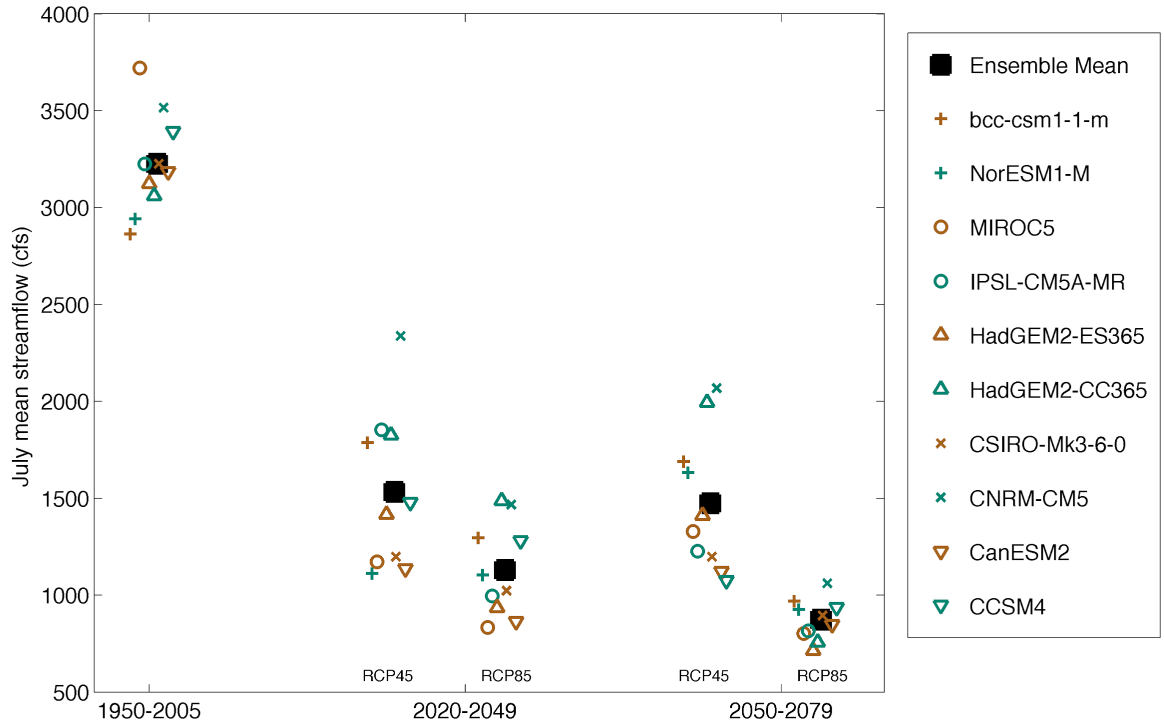

Figure 6.2: Modeled July mean streamflow in cubic feet per second for the Boise River near Lucky Peak under historical (left), early 21st century (middle) and mid-21st century (right) from 10 downscaled climate models for low emissions (RCP4.5) and high emissions (RCP8.5) scenarios. The black box shows the average of the 10 models.

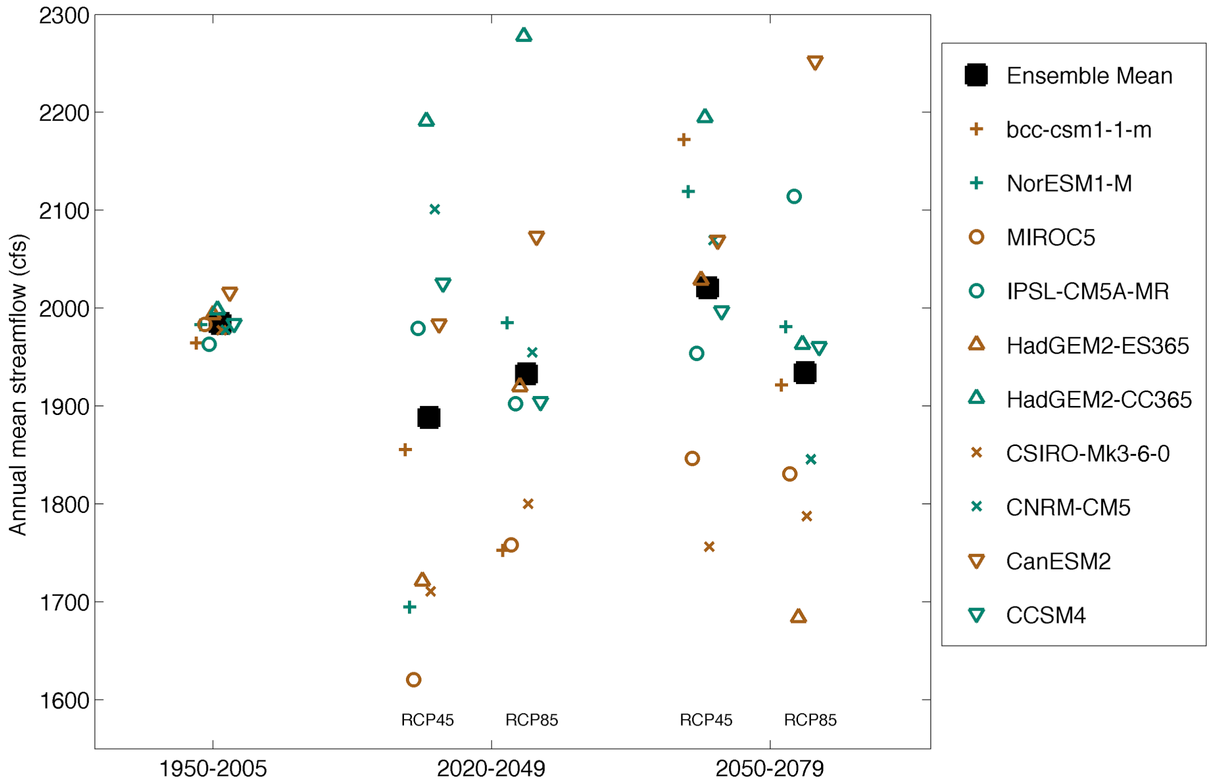

Figure 6.3: Modeled annual mean streamflow in cubic feet per second for the Boise River near Lucky Peak under historical (left), early 21st century (middle) and mid-21st century (right) from 10 downscaled climate models for low emissions (RCP4.5) and high emissions (RCP8.5) scenarios. The black box shows the average of the 10 models.

References

Liang, X., D. P. Lettenmaier, E. F. Wood, and S. J. Burges, 1994: A Simple hydrologically Based Model of Land Surface Water and Energy Fluxes for GSMs, *J. Geophys. Res.*, **99**(D7), 14415-14428

Lohmann, D., R. Nolte-Holube, and E. Raschke, 1996: A large-scale horizontal routing model to be coupled to land surface parametrization schemes, *Tellus*, **48**(A), 708-721

Metric VII: High streamflows and river flooding potential

Defined: High streamflow due to rapid snowmelt, heavy rainfall a combination thereof across upstream watersheds can pose a threat for flooding of the Boise River. Daily streamflow is monitored operationally by the National River Forecast Center and National Weather Service to alert for the potential for river flooding. The volume of water passing through a river or stream, often measured in cubic feet per second, that is also a proxy for river heights and scope of flood hazards. Natural flow refers to the natural runoff of a watershed or waterbody that would have occurred in the absence of human influences on the watershed. While the Boise River is heavily managed, we use naturalized flow as it more purely captured the influence of environmental change on water levels. Numerical values thus should not be directly compared with observed flow on the system. However, we emphasize that relative differences between baseline and future climate conditions should provide a measure of potential changes.

How it is calculated: Hydrologic models are used to simulate surface water dynamics including snowpack, soil moisture and runoff. The Variable Infiltration Capacity (VIC, Liang et al., 1994) model was used in this analysis given its widespread usage in climate-hydrology studies across the western US both operationally and for climate studies. The VIC model was done by the University of Washington as part of the USGS Northwest Climate Science Center funded Integrated Scenarios of the Future Environment project. These models used 10 of the aforementioned 20 downscaled climate scenarios (Table 7.1), and model processes including precipitation phase, snowmelt, and soil-vegetation interactions. A river routing scheme (Lohmann et al., 1998) was used to connect runoff from the upstream watershed to simulate river flow at various locations.

Data: Daily streamflow was obtained for 10 climate projections run through VIC for a location on the Boise River upstream of Boise near Lucky Peak Inflow. These data are for naturalized flow and do not account for upstream diversions, dam operations, etc. Given that the Boise River is heavily managed, it is not recommended to focus on the actual numbers, but rather differences between the scenarios and the historical baseline.

Analysis: Annual peak daily streamflow was examined separately for each of the 10 downscaled climate models for the historical modeled data (1950-2005) and future climate scenarios for the early (2020-2049) and mid-21st century (2050-2079). We also calculate the calendar day of the year coinciding with the annual peak flow to assess changes in the timing of peak runoff.

Results: No substantial changes in the magnitude of peak streamflow was simulated across models and scenarios (Figure 7.1; Table 7.1). The magnitude of peak flow is around 14,000 cubic feet per second for the simulations, which is would result in widespread flooding for the Boise River. However, the construction of Lucky Peak reservoir in 1946 mitigated flow risk and thus lower realized water levels. Hence, the focus should be on relative changes in flow between historical (1950-2005) simulations and future climate scenarios. While the models do not suggest a substantial change in the magnitude of peak streamflow, they do suggest a shift in the timing of peak runoff. Under the historical runs, the maximum daily streamflow occurs in June about 70%

of the time due to snowmelt runoff (Figure 7.2). The recession of mountain snowpack with warming leads to a substantial change in the timing of peak runoff with only 10% of peak daily streamflow occurring in June by the mid-21st century under high emission runs. Instead, peak daily streamflow is most likely to occur in May by the mid-21st century. Of additional interest is the increased occurrence of peak streamflow occurring from November-April under future climate scenarios. Under historical simulations, peak annual streamflow occurred in about 4% of runs during Nov-April, whereas 32% of years had peak annual streamflow in November-April for mid-21st century runs for high emission scenarios.

Summary: Human-caused climate change is not projected to significantly alter the magnitude of peak streamflow in the Boise River. However, a far greater proportion of high streamflow events are projected to occur during the fall through winter as a consequence of changes in snow and snowmelt timing on upstream watersheds and more winter precipitation falling as snow and directly running off. This is likely to result in a greater incidence of cool season floods along the Boise River.

Table 7.1: Average annual maximum daily streamflow (cubic feet per second) as simulated by the Variable Infiltration Capacity model for the Boise River near Lucky Peak for different climate models and time periods. Model output is for unregulated river, hence should be different than observed data.

	1950-2005	2020-2049 RCP45	2020-2049 RCP85	2050-2079 RCP45	2050-2079 RCP45
bcc-csm1-1-m	13742	12528	12226	14667	11667
NorESM1-M	14600	11890	15492	16431	15196
MIROC5	14136	9568	12634	11526	12201
IPSL-CM5A-MR	13670	13245	14173	13045	16243
HadGEM2-ES365	14393	11475	14052	13946	11802
HadGEM2-CC365	13887	16561	15910	15987	14206
CSIRO-Mk3-6-0	13149	11635	11919	11495	13174
CNRM-CM5	13034	14986	13014	13221	12375
CanESM2	13683	13420	14037	12527	16233
CCSM4	14056	13120	14015	14561	14043
MEAN	**13835**	**12843 (-6%)**	**13747 (-1%)**	**13741 (-1%)**	**13714 (-1%)**

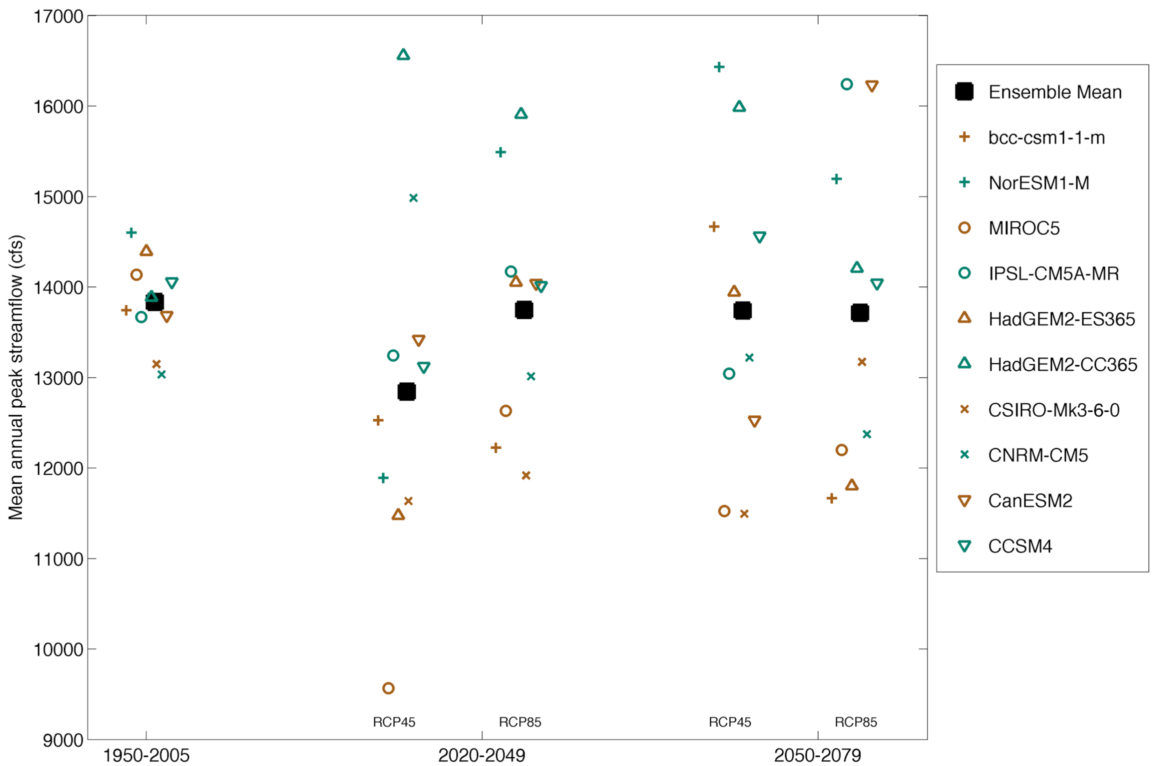

Figure 7.1: Modeled annual maximum streamflow in cubic feet per second for the Boise River near Lucky Peak under historical (left), early 21st century (middle) and mid-21st century (right) from 10 downscaled climate models for low emissions (RCP4.5) and high emissions (RCP8.5) scenarios. The black box shows the average of the 10 models.

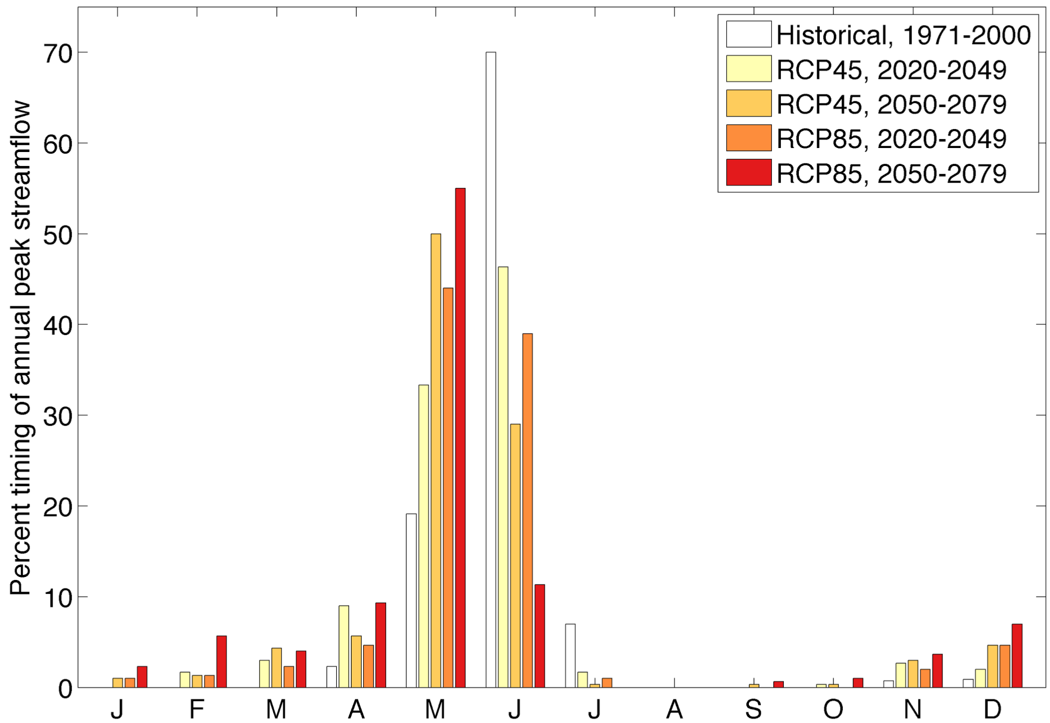

Figure 7.2: Seasonal timing of peak annual streamflow for the Boise River near Lucky Peak expressed as the percent of months during which peak streamflow was recorded for historical climate (white), early 21st century under low emissions (yellow), mid 21st century under low emissions (orange), early 21st century under high emissions (orange-red) and mid-21st century under high emissions (red).

References

Liang, X., D. P. Lettenmaier, E. F. Wood, and S. J. Burges, 1994: A Simple hydrologically Based Model of Land Surface Water and Energy Fluxes for GSMs, *J. Geophys. Res.*, **99**(D7), 14415-14428

Lohmann, D., R. Nolte-Holube, and E. Raschke, 1996: A large-scale horizontal routing model to be coupled to land surface parametrization schemes, *Tellus*, **48**(A), 708-721

Metric VII: Low streamflow and water quality issues

Defined: Low streamflows allow pollutants to concentrate and results in more volatile (mainly higher) water temperatures. Collectively, critically low water levels pose chronic impacts to aquatic life. The occurrence of low flows may also limit discharge into the water system thus impacting water treatment facilities. Low flows occur seasonally during periods of prolonged dry weather, most often during the late summer months in Idaho. Natural flow refers to the natural runoff of a watershed or waterbody that would have occurred in the absence of human influences on the watershed. While the Boise River is heavily managed, we use naturalized flow as it more purely captured the influence of environmental change on water levels. Numerical values thus should not be directly compared with observed flow on the system. However, we emphasize that relative differences between baseline and future climate conditions should provide a measure of potential changes.

How it is calculated: Hydrologic models are used to simulate surface water dynamics including snowpack, soil moisture and runoff. The Variable Infiltration Capacity (VIC, Liang et al., 1994) model was used in this analysis given its widespread usage in climate-hydrology studies across the western US both operationally and for climate studies. The VIC model was done by the University of Washington as part of the USGS Northwest Climate Science Center funded Integrated Scenarios of the Future Environment project. These models used 10 of the aforementioned 20 downscaled climate scenarios (Table 8.1), and model processes including precipitation phase, snowmelt, and soil-vegetation interactions. A river routing scheme (Lohmann et al., 1998) was used to connect runoff from the upstream watershed to simulate river flow at various locations. Low flows are defined by the 7Q10 which represents the 7-day average low flow with a return period of 10-years. The EPA uses 7Q10 and associated measures as a guide for water quality standards given that pollutants concentrate as water quantity declines.

Data: Daily streamflow was obtained for 10 climate projections run through VIC for a location on the Boise River upstream of Boise near Lucky Peak Inflow. These data are for naturalized flow and do not account for upstream diversions, dam operations, etc. Given that the Boise River is heavily managed, it is not recommended to focus on the actual numbers, but rather differences between the scenarios and the historical baseline.

Analysis: 7Q10 was calculated separately for each of the 10 downscaled climate models for the historical modeled data (1950-2005) and future climate scenarios for the early (2020-2049) and mid-21st century (2050-2079). This was accomplished by finding the annual minimum of 7-day average streamflow and estimating the 10-year return period using a percentile approach (e.g., the 10th percentile of annual 7-day mean low flow).

Results: Models project a decline in the magnitude of 7Q10 low flows under future climate runs (Figure 8.1; Table 8.1). Multi-model average decline in 7Q10 is 8% for the early 21st century and up to 15% by the mid-21st century. These results are directionally consistent with summer declines in streamflow, although are somewhat less extreme in magnitude. By comparison, the average decline in 7Q10 for 42-rivers across the northwestern US from 1948-2011 was 26.6% (Kormos et al., 2016). Declines in mountain precipitation over this period likely contributed to the declines in measured low flow values (e.g., Luce et al., 2013).

The declines in summer streamflow lead to a substantial increase in the frequency of low flow periods below present-day 7Q10 values. For example, an average of 44% of all summers had flows below current 7Q10 values for the mid-21st century under high emission scenarios. This represents a 300% increase in the frequency of such events.

Summary: Human-caused climate change is projected to result in further declines in low flows in the Boise River due to an advancement in the timing of mountain snowmelt, increases in evaporative demand, and the extended period of warm and dry conditions during the summer months. Conditions that are detrimental to water quality and aquatic life defined as being below current 7Q10 levels are expected to increase substantially, with a 300% increase in summer low flows meeting such criteria by the mid-21st century.

Table 8.1: Average annual maximum daily streamflow (cubic feet per second) as simulated by the Variable Infiltration Capacity model for the Boise River near Lucky Peak for different climate models and time periods. Model output is for unregulated river, hence should be different than observed data.

	1950-2005	2020-2049 RCP45	2020-2049 RCP85	2050-2079 RCP45	2050-2079 RCP45
bcc-csm1-1-m	345	355	311	308	287
NorESM1-M	354	323	284	329	301
MIROC5	368	329	323	345	306
IPSL-CM5A-MR	372	318	313	336	300
HadGEM2-ES365	320	300	320	342	297
HadGEM2-CC365	368	325	315	337	290
CSIRO-Mk3-6-0	350	323	316	300	302
CNRM-CM5	373	366	339	340	322
CanESM2	354	312	326	315	319
CCSM4	351	336	318	316	301
MEAN	**356**	**329 (-8%)**	**316 (-11%)**	**327 (-8%)**	**302 (-15%)**

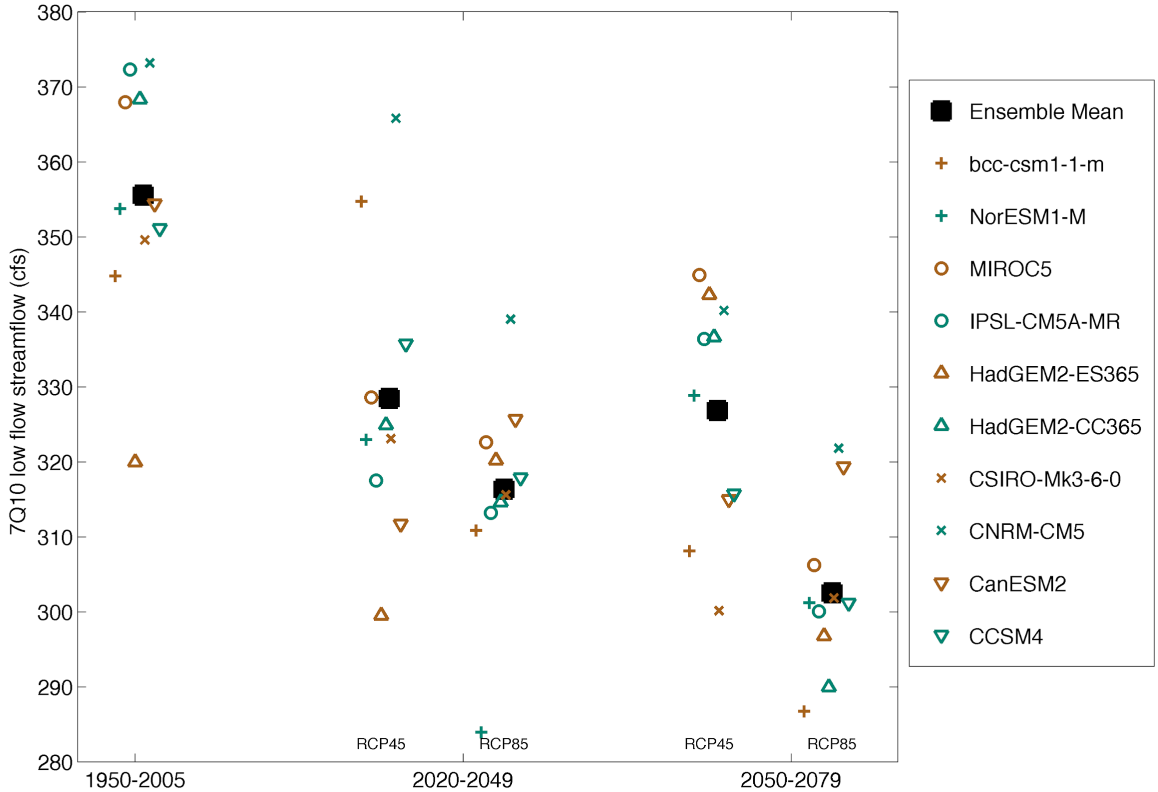

Figure 8.1: Modeled annual maximum streamflow in cubic feet per second for the Boise River near Lucky Peak under historical (left), early 21st century (middle) and mid-21st century (right) from 10 downscaled climate models for low emissions (RCP4.5) and high emissions (RCP8.5) scenarios. The black box shows the average of the 10 models.

References

Kormos, P. R., C. H. Luce, S. J. Wenger, and W. R. Berghuijs (2016), Trends and sensitivities of low streamflow extremes to discharge timing and magnitude in Pacific Northwest mountain streams, Water Resour. Res., 52, 4990–5007

Liang, X., D. P. Lettenmaier, E. F. Wood, and S. J. Burges, 1994: A Simple hydrologically Based Model of Land Surface Water and Energy Fluxes for GSMs, *J. Geophys. Res.*, **99**(D7), 14415-14428

Lohmann, D., R. Nolte-Holube, and E. Raschke, 1996: A large-scale horizontal routing model to be coupled to land surface parametrization schemes, *Tellus*, **48**(A), 708-721

Luce, C. H., J. T. Abatzoglou, and Z. A. Holden (2013), The missing mountain water: Slower westerlies decrease orographic enhancement in the Pacific Northwest USA, *Science*, 342(6164), 1360–1364

Appendix: Model Rankings

Global climate models (GCMs) are numerical models of climate system that include processes simulated by and between the atmosphere, ocean, land, ice and the biosphere. A coordinated set of experiments called the Coupled Model Intercomparison Project (CMIP) has been performed whereby models developed by various labs across the world perform common experiments as a means to compare results. We used models that took part in the most recent CMIP and used in the fifth assessment report of the IPCC. We considered three experiments: (1) historical simulations (covering the period from 1850-2005), (2) a low-emissions future from 2006-2099, and (3) a high-emissions future from 2006-2099. The latter scenarios are part of the Representative Concentration Pathway (RCP) experiments, which prescribe trajectories for the additional amount of energy trapped in the climate system as a result of increased greenhouse gas concentration. Specifically, the low and high emission pathways considered, RCP4.5 and RCP8.5, prescribe that an extra 4.5 and 8.5 Watts per meter squared are trapped in the Earth-Atmosphere system compared to a pre-industrial climate. For reference, man-made radiative forcing as of 2011 is approximately 2.2 Watts per meter squared more than pre-industrial times.

We chose models on the basis of them having available daily output for all variables as part of the downscaling process (http://maca.northwestknowledge.net), resulting in a total of 20 models. Mote et al., (2011) encourage climate impacts assessments to use at least 10-12 models, rather than rely on one or a handful of models. While a democratic system can be applied, where each model is treated as an equally likely outcome, there are differences in model credibly that could favor excluding certain models. Specifically, Rupp et al. (2013) examined the ability of climate models to simulate characteristics of climate across the broader northwestern US. This included the ability of models to capture the seasonal cycle of temperature and precipitation, 20th century trends, and large scale climate variability associated with the El Nino-Southern Oscillation. We provide a ranking of the subset of models from Rupp et al. (2013) that are used in this assessment to help assess any potential outliers. However, we note that model credibility over the historic time period does not necessarily provide information regarding the credibility of future projections.

Table A1. Attributes of CMIP5 global climate models and their ranking among the 20 from Rupp et al. (2013). Ranking of 1 indicates best, 20 indicates worst.

Model	Center	Ranking
BCC-CSM1-1	Beijing Climate Center, China Meteorological Administration	18
BCC-CSM1-1-M	Beijing Climate Center, China Meteorological Administration	12
BNU-ESM	College of Global Change and Earth System Science, Beijing Normal University, China	19
CanESM2	Canadian Centre for Climate Modeling and Analysis	2
CCSM4	National Center of Atmospheric Research, USA	5
CNRM-CM5	National Centre of Meteorological Research, France	1
CSIRO-Mk3-6-0	Commonwealth Scientific and Industrial Research Organization/Queensland Climate Change Centre of Excellence, Australia	8
GFDL-ESM2G	NOAA Geophysical Fluid Dynamics Laboratory, USA	14

GFDL-ESM2M	NOAA Geophysical Fluid Dynamics Laboratory, USA	10
HadGEM2-CC	Met Office Hadley Center, UK	4
HadGEM2-ES	Met Office Hadley Center, UK	3
INMCM4	Institute for Numerical Mathematics, Russia	11
IPSL-CM5A-LR	Institut Pierre Simon Laplace, France	13
IPSL-CM5A-MR	Institut Pierre Simon Laplace, France	6
IPSL-CM5B-LR	Institut Pierre Simon Laplace, France	20
MIROC5	Atmosphere and Ocean Research Institute (The University of Tokyo), National Institute for Environmental Studies, and Japan Agency for Marine-Earth Science and Technology	7
MIROC-ESM	Japan Agency for Marine-Earth Science and Technology, Atmosphere and Ocean Research Institute (The University of Tokyo), and National Institute for Environmental Studies	16
MIROC-ESM-CHEM	Japan Agency for Marine-Earth Science and Technology, Atmosphere and Ocean Research Institute (The University of Tokyo), and National Institute for Environmental Studies	17
MRI-CGCM3	Meteorological Research Institute, Japan	15
NorESM1-M	Norwegian Climate Center, Norway	9

References

Mote, P., L.Brekke, P. B.Duffy, and E.Maurer (2011), Guidelines for constructing climate scenarios, Eos Trans. AGU, 92(31), 257.

Rupp, D. E., J. T. Abatzoglou, K. C. Hegewisch, and P. W. Mote (2013), Evaluation of CMIP5 20th century climate simulations for the Pacific Northwest USA, J. Geophys. Res. Atmos., 118, 10,884–10,906